Universidade de Aveiro
2015

Departamento de Engenharia de Materiais e Cerâmica (DEMaC)

Aneeta Jaggernauth

Polymer Functionalization of Nano-Graphene Oxide by Molecular Layer Deposition

Dissertação apresentada à Universidade de Aveiro para cumprimento dos requisitos necessários à obtenção do grau de Mestre em Engenharia de Materiais realizada sob a orientação científica da Doutora Mercedes Vila Juarez, Investigadora Principal de Departamento de Engenharia Mecânica e coorientação do Professor Doutor Rui Ramos Ferreira e Silva, Professor Associado do Departamento de Engenharia de Materiais e Cerâmica da Universidade de Aveiro

O Júri

Presidente	Doutora Paula Celeste da Silva Ferreira. Equiparada a Investigadora Principal, Universidade de Aveiro
Vogal - Arguente Principal	Professora Doutora Florinda Mendes da Costa. Professora Associada, Universidade de Aveiro
Vogal - Orientador	Doutora Mercedes Vila Juarez. Equiparada a Investigadora Principal, Universidade de Aveiro

Acknowledgements

The work presented here is the result of the involvement and influence from a special group of individuals, who have unfailingly devoted their time and scientific guidance to the success of this endeavour. I therefore extend to them my sincere gratitude and honour their valuable contributions.

Firstly, I am immensely thankful to my supervisors and mentors, Dr. Mercedes Vila Juarez and Professor Rui Ramos Ferreira e Silva for their guidance, expertise, support, and enthusiasm imparted from inception, and serving as a beacon throughout this experience.

I am also grateful to Gil Gonçalves, Filipe Oliveira, Miguel Angelo Neto, Maria Jesús Hortigüela, and Ricardo Silva who have graciously and patiently shared their superior knowledge in their respective fields, and without whom the practical work necessary to fulfil this undertaking would not be realized.

Finally, I would like to express my gratitude to Maria Celeste Azevedo, Ana Ribeiro and Narendar Nasani, who were instrumental not only in performing characterization techniques, but doing so in a timely manner and welcoming dialogue for enhancing understanding.

Palavras-chave molecular layer deposition, graphene oxide, polyethylene glycol, nanoparticle functionalization, nanocomposite, hybrids

Resumo

O presente trabalho aborda o processo de funcionalização por via seca de nanopartículas de óxido de grafeno (nano-GO) visando o estabelecimento de ligações a polietilenoglicol (PEG) na sua superfície. Atualmente utilizam-se métodos químicos de funcionalização por via húmida com esta finalidade, no entanto são demorados e resultam em perdas significativas de amostra. O trabalho foi realizado em duas fases: o GO foi primeiramente sintetizado em forma de filme e pó utilizando um método "Hummers" modificado, sendo caracterizado por FTIR, SEM e DLS; em seguida o GO foi exposto aos precursores do PEG num reator de deposição por camada molecular (MLD) sob condições de vácuo. Utilizaram-se temperaturas diversas de deposição, tendo-se observado uma adsorção ótima entre 90-100° C. Primeiramente, a deposição de PEG em pó de GO, com terminações de amina, confirmou por FTIR a presença dos picos característicos de PEG, aproximadamente aos 2925 cm^{-1} e 2850 cm^{-1}, corroborando a funcionalização a seco do GO por um mecanismo de vaporização-condensação. A via MLD, usando TMA e EG como precursores foi então realizada no pó de GO, tendo proporcionado uma camada de passivação inicial rica em alumínio, na qual ciclos subsequentes de exposição ao monómero EG resultaram na sua adsorção e polimerização, tal como demonstrado por FTIR e análises EDS.

O nano-GO-PEG é vantajoso para aplicações na área da biomedicina, incluindo sistemas de administração de fármacos, biossensores e terapia fototérmica. O PEG permite ao nano-GO ser reconhecido como biocompatível, estabelecendo uma superfície repelente e incrementando o transporte citoplasmático, permitindo assim características essenciais, tais como alta absorvância óptica, fluorescência e estabilidade em meio fisiológico, essenciais para os sistemas biológicos. O sucesso da produção do nano-GO funcionalizado com PEG pela via a seco aqui proposta poderá será favorável para outros tipos de funcionalização e copolimerização de nanopartículas.

Keywords molecular layer deposition, graphene oxide, polyethylene glycol, nanoparticle functionalization

Abstract

This research aims to achieve a dry functionalization approach for covalently attaching polyethylene glycol (PEG) onto the surface of nano-graphene oxide (GO). Currently, wet chemical methods are used to achieve this, being characteristically time consuming and resulting in significant loss of sample. This work is carried out in two stages; GO is first synthesized using a modified Hummers' method, and then characterized by FTIR, SEM and DLS; it is then produced in film and powder form, for exposure to precursors in an MLD reactor under rough vacuum conditions. GO films were exposed to PEG at variable temperatures, determining that at 90^{o}C and 100^{o}C the optimal adsorption occurred. Deposition of amine-terminated PEG on GO powder confirmed the presence of characteristic PEG peaks around 2925cm^{-1} and 2850cm^{-1} via FTIR, substantiating the dry functionalization of GO via vaporization-condensation. An MLD route, using TMA and EG precursors was then performed on GO powder, delivering an initial passivation layer of Al, onto which subsequent cycles of EG adsorbs, demonstrated by FTIR and EDS analysis.

PEGylated-nano-GO is advantageous for applications in the area of biomedicine; including drug delivery systems, biosensors and photothermal therapy. PEG permits nano-GO to be recognized as biocompatible; establishing on it a non-fouling surface and increasing its cytoplasmic transport, thereby allowing its inherent characteristics such as high optical absorbance, fluorescence, and stability in physiological media to be pertinent to biological systems. Successful production of PEG functionalized nano-GO via the proposed method will be favourable for other possibilities of nanoparticle surface functionalization and copolymerization.

Table of Contents

List of Figures

CHAPTER 1 INTRODUCTION

1.1. Motivation and Objectives

This work was carried out to establish a fast, dry method approach for attaching polyethylene glycol (PEG) onto the surface of nano-graphene oxide (GO), using molecular layer deposition (MLD) to attain molecular control over this functionalization. Currently, GO surface functionalization with PEG is normally achieved using wet chemical processes, which are relatively lengthy because of their required purification and results in noticeable sample loss. These processes involve the use of carbodiimide compounds such as EDC 1-ethyl-3-(-3-dimethylaminopropyl) carbodiimide hydrochloride, which functions as a crosslinker between carboxyl groups present on the surface of the GO and primary amine groups, which terminate the PEG polymer chain.

The last 10 years has seen significant advancement in the synthesis and applications of graphene based materials, including graphene, graphene oxide and reduced graphene oxide. These materials have been functionalized with metallic and organic atoms to be used in a variety of applications such as transparent electrodes for LED and solar cell devices, high capacity energy storage in lithium batteries and in biomedical applications. It is for this last application that the surface functionalization of GO with PEG is essential for use as drug delivery vehicles, imaging and sensor devices, and to effect cell death via laser ablation.

The dry method approach used for GO functionalization with PEG is that of molecular layer deposition (MLD), a variation of atomic layer deposition (ALD), a method typically used for the growth of metal oxide very thin films with atomic level control. MLD produces uniform and conformal ultra-thin films (typically below 100 nm in thickness) driven by a sequential and self-limiting layered deposition with molecular level control. Recent advances in molecular layer deposition (MLD) include the coating of nanoparticles with hybrid films, such as alucones; polymeric aluminium alkoxides with carbon-containing backbones, produced by layers of aluminium oxide (inorganic) and an organic component such as ethylene glycol.

MLD will be a novel approach. To date there is no literature that addresses the controlled functionalization of GO with PEG molecules via MLD. The very few published papers which tackle ALD onto graphene oxide, focus on the decoration of GO with Pt for use in gas sensors, and also on its functionalization with metal oxides; alumina and zirconia[1].

The achievement of a faster and optimized option is desirable, being obviously advantageous to researchers, curtailing the time needed to obtain PEGylated GO with high purity, to be used in its variety of applications, but also on a more substantial scale as it applies to the commercialization of this material. Equally, if not more, important are the possibilities presented for nanoparticle surface functionalization and control at the molecular level that is, the length of the polymer chain; initiatives for copolymerization of GO surfaces, as well as hybrid functionalization are necessary for manipulating the properties of GO or lending them to their attached counterparts.

1.2. Literature Review

1.2.1 Structure and Properties of Graphene and Graphene Oxide

Graphene has established itself as a material at the forefront of many research areas such as microelectronics, biomedical and bioengineering, and energy efficient technology, due to it possessing the following properties; specific surface area of $2630 m^2 g^{-1}$, charge mobility of $2x10^5 cm^2 V^{-1} s^{-1}$, Young's modulus of 1.0TPa, thermal conductivity of $5000 Wm^{-1} K^{-1}$, and optical transmittance of 97.7%; all considered to be relatively high values of the respective properties[2].

These properties are the result of the structure of graphene which is described by a single atomic layer of sp^2 carbon atoms densely packed into a hexagonal planar lattice. Each carbon atom has four valence electrons; three forming covalent σ bonds responsible for the rigid in-plane structure, and the fourth forming π bonds, distributed equally along three directions, controlling the interaction between graphene layers (Figure 1)[3]. Bonding in graphene allows the material to exhibit both continuous layers of delocalized electrons and rigid covalent bonds, so that it is able to disperse phonons efficiently across it while withstanding sufficient stretching thus making it one of the strongest known materials[4].

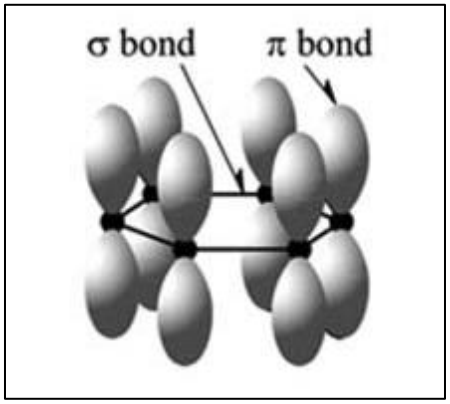

Figure 1: Structure of graphene showing σ bonds lying in plane and π bonds perpendicular to the plane[3].

The π bonds in graphene contribute to delocalized electrons which affects the interaction between layers of graphene sheets. A single sheet is defined as a 2-dimensional sheet of hexagonally arranged carbon atoms; graphene, and is more difficult to produce than multiple layer sheets. Bi-layer sheets refer to 2 sheets, few-layer sheets are those between 3 to 10 sheets and anything over 10 are considered to be thick sheets; graphite, used in lubricants and pencils because of the ease at which slipping of their sheets occur, and also in the use of refractories because of their chemical resistance, thermal conductivity and hot compressive strength.

Chemically modified graphene (CMG), rather than graphene, has also been studied for applications such as polymer composites, energy-related materials, sensors, and biomedical applications, due to its excellent electrical, mechanical, and thermal properties[5]. CMGs can be obtained by covalent or non-

covalent bonding, so that surface modified graphene, sheet blends and even 3-dimensional materials, formed by controlling the interactions between sheets, can be obtained[5]. Graphene oxide (GO) offers possibilities for the production of CMGs as it contains a range of reactive oxygen functional groups, making it a versatile material for this purpose.

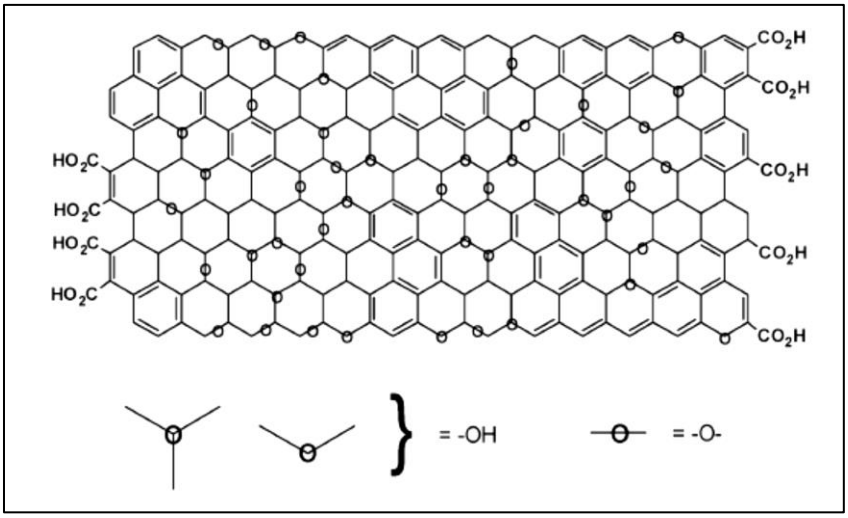

Figure 2: Structure of graphene oxide showing allocation of groups in the basal planes and on the edges of a GO sheet[6].

Graphene oxide is synthesized by the chemical exfoliation of graphite to weaken the Van der Waals interactions between the stacked carbon sheets[7]. Nano-GO can further be obtained from the lateral breaking of micro-sized GO to that of the nano-sized range; being considered as a plane of hexagonally structured carbon atoms having carboxylic and carbonyl groups on its edges, and hydroxyl and epoxy groups on its basal planes, as seen in Figure 2. The benefit of forming nano-GO is its versatility derived from the presence of a high density of functional groups, and also because of its high aspect ratio[7], alluding to its high rate of functionalization and interaction, which is desirable especially for cell uptake and therefore biological applications.

1.2.2 Graphene Oxide Synthesis

The top-down approach is one of the most used for the synthesis of graphene based materials. The most common is the chemical exfoliation of graphite, a process involving the use of chemical energy to break the Van der Walls bonds between the layers, eventually resulting in individual or few sheets-thick of graphene oxide.

Hummers' method for the synthesis of graphite oxide from graphite, was reported in 1958 by Hummers and Offeman[8]. It provided a faster and safer method than that reported by Staudenmaier in 1898[8], replacing the explosive potassium chlorate required, with potassium permanganate, lowering the temperature, and shortening the time for which the reaction would occur.

The Hummers' method involves the oxidation of graphite by reacting $KMnO_4$ (potassium permanganate) and $NaNO_3$ (sodium nitrate) in concentrated H_2SO_4 (sulphuric acid). The reaction between the $KMnO_4$

and H_2SO_4 results in the production of MnO_7 (dimanganese heptoxide)[6], shown in equations (1)[6] and (2)[6], which is very reactive and therefore acts to oxidize the graphite.

$$KMnO_4 + H_2SO_4 \rightarrow K^+ + MnO_3^+ + H_3O^+ + 3HSO_4^- \quad (1)$$

$$MnO_3^+ + MnO_4^- \rightarrow MnO_7 \quad (2)$$

It has the effect of intercalating the graphite layers with oxygenated functionalities or moieties increasing the interlayer spacing from 0.34nm to approximately 0.6nm[8,9], resulting in graphene oxide, identified by many expanded layers, intercalated with oxygenated moieties such as carbonyl, carboxyl, hydroxyl and epoxy groups[10].

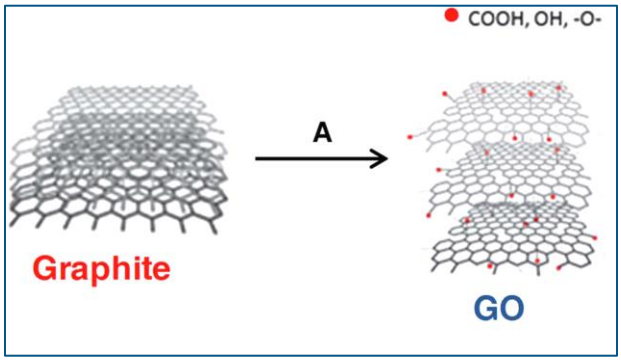

Figure 3: Hummers oxidation of graphite to form graphene oxide (GO); 'A' representing reaction with $NaNO_3$, H_2SO_4 and $KMnO_4$, followed by H_2O_2[11]

The expanded nature of graphite oxide makes its layers susceptible to exfoliation to obtain a single or few-layer material, shown in Figure 3. Separation of the sheets can be achieved by the decomposition of the functional groups to produce a large amount of gas in the Van der Waals space, by chemical or thermal means, the gas over-pressure resulting in the splitting of the layers to form few or single layers[10]. Ultra-sonication can also be used for breaking apart the layers to create micro-graphene oxide, with further breakage leading to nano-GO. The degree of oxidation creates defects in the material subsequently forming cracks and their propagation upon ultra-sonication, thereby controlling the lateral size of the GO sheets[7].

GO, having a variety of functional groups, can be surface activated to possess only the desired oxygen moieties for its purpose, for example activation with carboxyl groups via chloroacetic acid and sodium chloride. This results in the occurrence of only COOH functional groups at the surface of GO. These carboxyl sites can and have been used to immobilize or conjugate proteins, polymers, targeting agents and antibodies[12].

1.2.3 Structure and Properties of Polyethylene Glycol

Polyethylene glycol (PEG) is a linear or branched polyether typically terminated with hydroxyl groups, having the structure H-(O-CH_2-CH_2)$_n$-OH. It is the result of the polymerization of ethylene glycol (EG) or the reaction of ethylene oxide and water. PEG may be hetero or homobifunctionalized, so that it possesses desired functional end groups, more suited to its use. Homobifunctionalized PEG with amine groups is typically used for binding with carboxyl groups.
Figure 4 shows structures of EG (monomer) and bi-functionalized PEG having different terminating groups R_1 and R_2. PEGylation of the nanoparticle occurs with one of the PEG end groups, R_1, attached to the particle and the other free to attach to another structure including enzymes, peptides and targeted molecules.

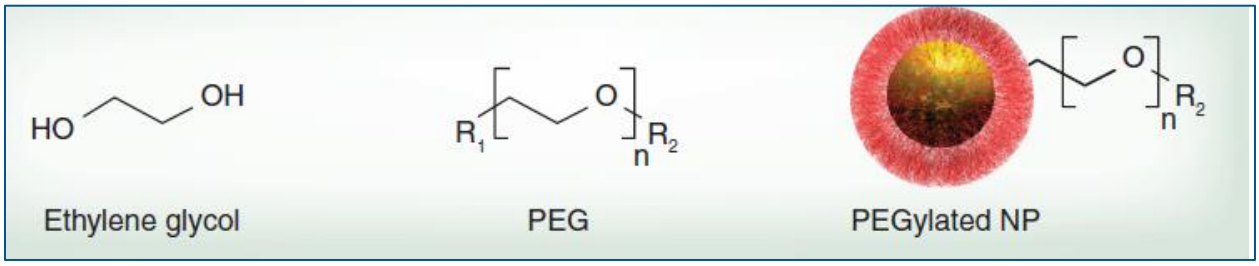

Figure 4: Structures of ethylene glycol (EG), hetero bi-functionalized PEG and a nanoparticle functionalized with PEG[13].

PEG has emerged as a beneficial material for conjugation with polypeptides, used in therapeutic applications, as it improves their pharmacokinetic and pharmacodynamic properties thereby preventing typical problems of a short circulating half-life, immunogenicity and low solubility[14]. PEG, when conjugated to GO, acts as a non-fouling agent to modify the GO surface so as to prevent protein attachment thereby hindering the action by immune responses of the body, registering it as a non-foreign object, consequently lowering the reticuloendothelial system (RES) clearance (opsonisation)[7,14]. This is possible because PEG is soluble in aqueous solutions, typically binding 2 to 3 water molecules per ethylene glycol unit[14]. It therefore creates a hydrophilic, non-fouling surface for the nano-GO in the form of a large flexible protein molecule. This functionalization of nano-GO with PEG, or PEGylation, increases its biocompatibility, making it highly stable in aqueous solution and susceptible to cell internalization.

1.2.4 Applications of PEGylated-GO in Biomedicine

Nano-GO, on its own also exhibits properties which make it impressive for biomedical and pharmaceutical applications. One example of this is seen by its high optical absorbance in the near infra-red (NIR) region, which is referred to the therapeutic or tissue transparency window (700-900nm) because of its non-invasive and harmless, but skin penetrating ability[7]. This absorbance is due to the aromatic structure of nano-GO. Covalent bonding with PEG allows for its increasing stability in an aqueous medium, improving its biocompatibility.

An application of this property of optical absorbance in the NIR region is photothermal therapy for the laser ablation of cancer cells, whereby the PEGylated nano-GO (nano-GO-PEG) acts as photo-absorbing agents for using optical energy to generate heat. Yang et al[15] successfully demonstrated this therapy in tumours of mice, they being injected intravenously with 2mg/ml nano-GO-PEG and the tumour subject to NIR radiation of 808nm and radiative flux 2W/cm^2, causing its elimination via hyperthermia[16]. It was however determined that a high radiative flux also disseminated heat to surrounding normal tissue, sufficient for cell damage or destruction, and as such the use of a lower irradiance should be investigated. In so doing Yang et al[15] determined that for an ultra-low flux of 0.15W/cm^2 reduced nano-GO-PEG, but not nano-GO-PEG, was successful in eliminating the tumour.

Nano-GO has also been held as a material which contributes beneficially to biosensor and imaging applications. The photoluminescence of nano-GO has been attributed to the oxidation of graphite, which causes disruptions in the planar sheets of GO causing electron-hole pair recombination localized in a sp^2 carbon domain which is further localized in a sp^3 matrix[17]. Other beneficial properties for these applications include its ability to become biocompatible and its heterogeneous structure, possessing functional groups on its edges and basal planes, which further contribute to its fluorescence.

Fluorescence Resonance Energy Transfer (FRET) is a phenomenon in which non-radiation energy is transferred from a donor molecule or fluorophore to an acceptor molecule, resulting in a decrease in the donor's fluorescence intensity and an increase in the acceptors emission intensity. This transfer of energy is dependent on the distance between the donor and acceptor pairs, typically being between 20-60Å[17]. FRET has been used for determination of the chemical structures of biological molecules and their interactions and for in vivo monitoring in cellular research[17,18]. Nano-GO has been tested, in different cases, as the donor and acceptor molecules for FRET. The non-covalent π-π stacking between nano-GO and DNA and peptides, makes nano-GO-PEG advantageous as an acceptor molecule and its high aspect ratio contributes a large number of acceptor molecules to FRET[17].

PEGylated nano-GO has also had success as a drug carrier due to it being biocompatible and stable in physiological fluids, including serum. It is especially advantageous for the delivery of water insoluble drugs, once they can be appropriately attached, making them soluble in an aqueous medium. An example of this was carried out with SN38, an aromatic molecule insoluble in water, and a camptothecin (CPT-11) analogue, an anticancer chemotherapy drug[19]. The attachment of SN38 to nano-GO-PEG was suggested to be non-covalent and as a drug delivery system, it was found to be water soluble for SN38 concentrations of about 1mg/ml[19]. CPT-11 would normally have to be metabolized to SN38 after administration in order to be activated, with a significant amount of it being excreted before metabolism, or metabolized to inactive compounds, but overcoming the insolubility of SN38 in water provides avenues for its direct use[19].

1.2.5 Wet Chemical Surface Functionalization

Functionalization of GO with PEG occurs via a wet chemical method. It is desirable to start with GO that has been activated with –COOH (carboxylic groups), which can be achieved by mixing and sonication with NaOH and chloroacetic acid as shown in Figure 5.

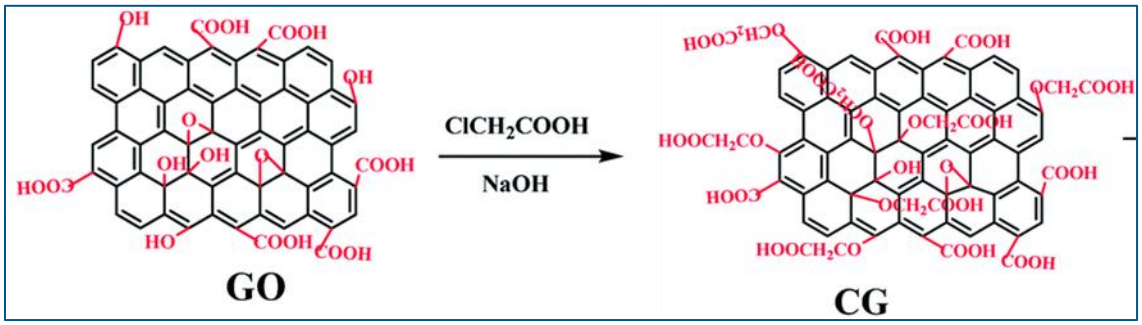

Figure 5: Activation of GO with COOH groups[20].

Functionalization of GO is then carried out on the activated GO with carbodiimide compounds, EDC 1-ethyl-3-(-3-dimethylaminopropyl) carbodiimide hydrochloride, a water soluble compound[20–22]. EDC is a crosslinker which activates carboxyl groups, in this case, present on GO, to bind with primary amine groups, found on PEG. This results in an amide bond being formed between the primary amine and the carboxyl group (Figure 6). The final structure carries no portion of the carbodiimide, so that they are considered to be zero-length carboxyl-to-amine crosslinkers[23].

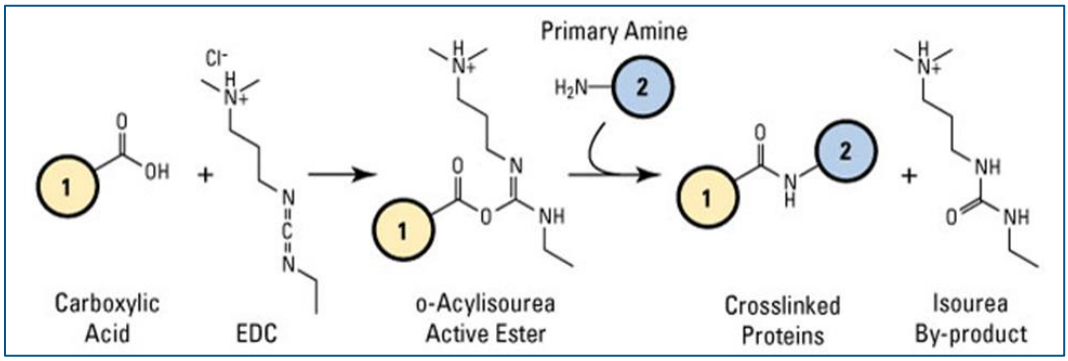

Figure 6: Crosslinking facilitated by EDC, between amine and carboxyl functional groups. '1' and '2' represent proteins, peptides or any chemicals having these end groups[23].

An important consideration for this research is the time needed for the wet chemical activation and PEG functionalization of GO. Articles have shown that this process can easily take 2 days for the addition of reactants and aging of the suspension[15,22,24,25]. Subsequent neutralization and purification necessary for COOH activation, dialysis or washing by centrifugation with filters for PEG functionalization, can take weeks until completion. Labelling of nano-GO-PEG with dyes, should it be required for the particular experiment, is also time-consuming, obliging numerous washes, to obtain solutions with no further changes in colour[22]; this process typically taking one week until completion.

It is the expectation that the time for these lengthy processes can be significantly truncated with the use of molecular layer deposition (MLD), a dry process in which time is dependent on the number of layers of molecules to be deposited on the surface of the material. Achievement of this would be beneficial in reducing the time for experimental work and also for the commercialization of functionalized GO.

1.2.6 Molecular Layer Deposition (MLD)

The atomic layer deposition (ALD) technique was brought about in response to the miniaturization of semiconductors and the popularity of microelectronics, and subsequent attractiveness of nanoparticles. It enabled continuous and conformal coating of nanoparticles and porous materials, with atomic control, producing thin films onto materials with high aspect ratios. Molecular layer deposition (MLD) is a variation of ALD to incorporate molecular layer control of uniform, continuous, conformal coatings. It is typical that ALD be performed for the creation of films of metal oxides, metal nitrides and other inorganic materials[26], while MLD allows for the deposition of organic molecules to create organic-organic or organic-inorganic (hybrid) layered films. Both techniques are carried out in a vacuum and must achieve film growth by sequential and self-limiting surface reactions.

The concept of MLD is shown in Figure 7. The schematic demonstrates the use of 2 precursors which will react to form the composition of the desired film on a flat substrate. The first precursor will sequentially deposit one layer of the first molecule (Figure 6(a))[22]. The self-limiting nature of MLD means that once the layer is deposited, this molecule will no longer be deposited as all the available sites on the substrate have already been filled, and the functional groups on the molecule will not allow for adsorption of the same molecule. A purging step is consequently performed to remove any remnants of the molecule or by products of the deposition before the second precursor is streamed into the vacuum chamber. This precursor supplies the second molecule which adsorbs onto the first, sequentially (Figure 6 (b)), and once again promotes a self-limiting reaction. Purging is again performed and the steps repeated until the desired layer thickness is achieved.

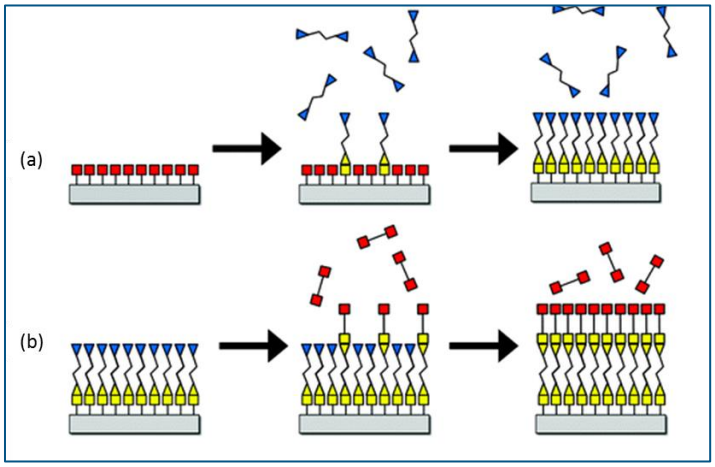

Figure 7: MLD - demonstration of the sequential deposition of a film with molecular layer control using two precursors to deposit different molecules[22]; the first shown in (a), the second in (b). A purging step is performed between the precursor steps[26].

MLD using only organic precursors was developed from an earlier gas phase polymer growth technique called vapour deposition polymerization (VDP), which created the co-evaporation of two types of bifunctional monomers under vacuum conditions[27]. MLD also uses bifunctional monomer precursors of

the form X-A-X and Y-B-Y, X and Y being chemical functional groups and A and B being the organic fragments. The chemical reactions corresponding to the steps shown in Figure 6 are therefore given by:

$$SBY^* + XAX \rightarrow SB - AX^* + XY \quad (3)$$

$$SAX^* + YBY \rightarrow SA - YB^* + XY \quad (4)$$

S represents the substrate and the deposited film and * denotes the surface species. Reactions (3) and (4) can therefore correspond to either (a) or (b) of Figure 6, depending on which precursor was used first.

1.2.7 MLD onto Nanoparticles

The deposition of films via MLD onto the surface of flat substrates is less challenging than that of powders, especially in the form of nanoparticles. The increased complexity of the shape, tendency to agglomerate and motion under vacuum conditions require the consideration and examination of some specific parameters. The benefit of coating nanoparticles of different shapes, including powders and tubes, is the modification it allows the surface properties, while maintaining those of the materials onto which it is deposited[28]. This is evident in the case of GO and its nano-sized counterparts, where, as was discussed above, its functionalization with PEG imparts biocompatibility and stability in aqueous and organic media, while maintaining the desired properties of the GO, in the case of its absorbance and fluorescence, for example.

The deposition of thin films onto powders and nanoparticles via MLD has been investigated using organic precursors[29,30], as well as organic-inorganic ones to obtain hybrid films[26–28,31]. Metal alkoxide polymeric films, called 'metalcones', are examples of organic-inorganic films grown from metal precursors and organic alcohols. Most popular are the 'alucones', grown from ethylene glycol (EG) and trimethylaluminium (TMA) precursors, but there are also 'zincones' and 'titanicones', resulting from organic diols and the corresponding metal precursor, such as diethylzinc (DEZ) and titanium tetrachloride ($TiCl_4$), respectively. The benefit of these films is the tunablity of their properties resulting from hybrid effects, impacting properties such as density, elastic modulus, hardness and refractive index[27].

The time taken for deposition of these hybrid films attest to the efficiency and relative rapidity of MLD. Large scale MLD onto SiO_2 and TiO_2 nanoparticles of approximate diameters of 250nm and 150nm, respectively, was performed with hybrid aluminium alkoxide (alucone) polymer films[28]. The precursors used were trimethylaluminium (TMA) and ethylene glycol (EG), which were incorporated with N_2 purging and evacuation after each precursor exposure. The conformal nature of the coatings on both silica and titania nanoparticles were confirmed, realizing growth rates of approximately 0.5nm/cycle at 100°C and 0.35nm/cycle at 160°C, respectively[24]. MLD of alucone films were also deposited onto flat Si substrates for which cycle times of 242s realized a thickness of just under 400Å after 100 cycles[31].

Inorganic films were also grown via MLD. A film of polyamide nylon (nylon 66) was deposited onto SiO_2 powder using adipoyl chloride (AC) and 1,6-hexanediamine (HD) bifunctional monomers of the form

ClCO-A-OCCl and H_2N-B-NH_2[29]. Both precursors required heating at temperatures of 50° and 38° for AC and HD, respectively[29], to create vapour pressure in order to obtain flow. The maximum time for completing one cycle of precursor A-purge-precursor B-purge was 700s, with an estimated growth of 19Å per cycle[29].

Much of the research published about dry functionalization of graphene-based materials has addressed ALD onto graphene to achieve surface functionalization while preserving its electronic properties, or to create free-standing films once the graphene is etched away. It was determined that some form of surface treatment prior to ALD was necessary for the proliferation of coatings. To achieve this, NO_2 or O_3 with TMA, for Al_2O_3, is used to provoke a seed layer onto which the ALD Al_2O_3 can be deposited[32–34]. TMA and water are typically used precursors for ALD of Al_2O_3 but the use of O_3, for example, in place of water is shown to create physisorbed oxygen species with short resident life times on the surface of the graphene which facilitates growth of the alumina coating[33]. Seed layers for graphene have also been achieved with inorganic films such as alkyl amine, poly4-vinylphenol and polyvinyl alcohol, non-covalently bonded to the graphene surface[1].

Specifically for graphene oxide, there is even less literature about dry functionalization of its surface. One paper discusses an ALD approach to decorate GO with Pt catalysts to increase the catalytic activity toward acid electrolytes, in this case, the electro-oxidation of formic acid[35]. ALD reviews have also highlighted depositions onto CNTs and graphene, with MLD being discussed in its value to metalcones and hybrid coatings, and graphene oxide barely being mentioned. The use of MLD for the functionalization of GO with PEG will therefore be quite novel.

On average the time taken for MLD surface functionalization with polymers and hybrid films, as discussed previously, is significantly less than that described above for wet chemical functionalization of GO with PEG, the benefit of this approach being sufficiently evident in this sole fact. Undertaking this approach requires consideration of factors such as the temperature of the precursors, their residence times, the suitability and efficiency of the sample holder and the temperature of deposition. Ethylene glycol (EG) for example is heavy and sticky and can easily be deposited onto the walls of the vacuum chamber rather than on the nanoparticles, if the temperature and residence times are not aptly chosen to permit simultaneous reaction and movement through the ALD chamber. The use of the EG monomer is necessary for control of the eventual constructed polymer as the nanocomposite size is important for cell uptake and therefore biological applications.

Success in the MLD approach for functionalization of GO brings with it possibilities for the creation of other nanocomposites and the functionalization of metallic and organic surfaces. Examples of this include PEGylated poly-lactic-co-glycolic acid (PEG-PLGA), which is used as a drug delivery system for the sustained release of anticancer drugs[36], and the PEGylation of gold nanoparticles also used for drug delivery but also in imaging; CT and radiograph contrast, and phototherapy[37].

CHAPTER 2 EXPERIMENTAL PROCEDURE

2.1. Synthesis of Surface Activated Graphene Oxide

2.1.1 Synthesis of Nano-Graphene Oxide

The synthesis route is shown in Figure 8 and the procedure is described below.

GO was synthesized from graphite using a modified Hummers method. 1g of graphite powder (Aldrich 496596, < 45μm, >99.99% purity) was mixed with 0.76g sodium nitrate ($NaNO_3$) (Sigma-Aldrich S5506, Reagent Plus ≥99.0%) in a flask, which was placed in an ice bath. 35ml sulphuric acid (H_2SO_4) was added and stirred at a speed of about 1000rpm, until homogenized. 4.5g $KMnO_4$ (Panreac 13157 PA-ACS, M=158.04, >99.0%) was then added, in four parts, over the course of 1 hour. After 2 hours the flask was taken out of the ice bath, and remained stirring for 7 days.
500ml H_2O and 25ml H_2SO_4 were mixed together until homogenized. The resulting brown slurry, obtained after ageing for 7 days, was then added to the 5wt% H_2SO_4 aqueous solution over the course of 1 hour (about 40ml added every 10 minutes), while being stirred. Stirring continued for an additional 2 hours after the last of the slurry was added. 100ml aqueous solution of 30wt% H_2O_2 was slowly added after the 2 hours, resulting in a change in colour of the slurry from brown to yellow. This resulting slurry was left stirring for 2 hours. 500ml H_2O, 15ml H_2SO_4 and 2.5ml H_2O_2 were mixed together and added to the yellow mixture, and stirred for 2 days.

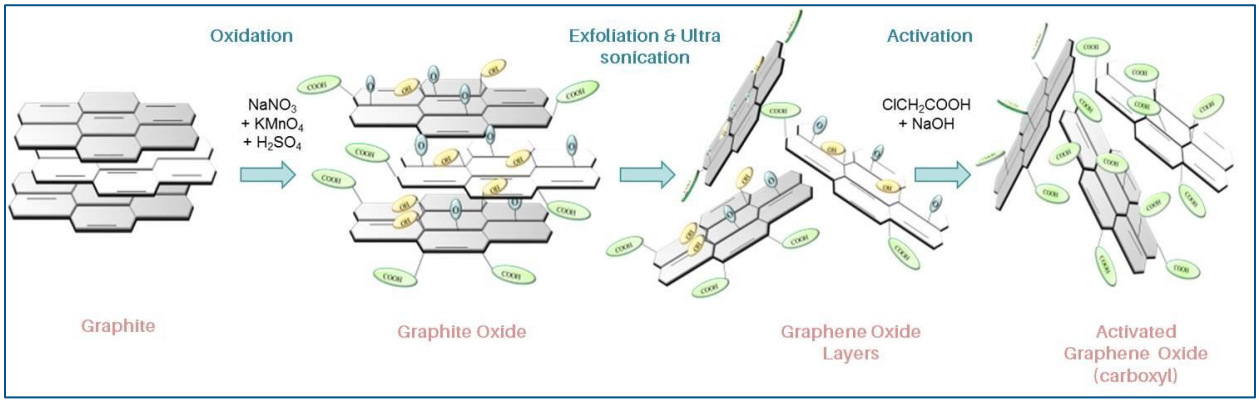

Figure 8: Synthesis route for GO activated with carboxyl groups (GO-COOH)

After 2 days the supernatant was removed. This was achieved by filtering the resulting mixture using filter paper under vacuum. Filtering was done with small volumes of the slurry because of the size of the filter and the time taken for filtering. When all the clear liquid (water and salts in solution) had been filtered into the flask and the brown precipitate remained on the filter paper, the vacuum was detached from the flask and the filter paper removed. The paper with the precipitate was placed in a beaker with about 500ml Milli-Q water and stirred with a magnetic stirrer until all the precipitate left the paper. The

paper was removed and more water was added to the beaker, until about 900ml. This was then sonicated for an hour, allowed to rest for an hour and then sonicated again. This process continued until the total volume of the slurry had been filtered, and then repeated 5 more times on the total volume. The initial and precipitated slurries remained stirring for the duration of the process.
When all the washes were completed, the resulting mixture was allowed to stand to precipitate. Once this occurred, the top layer, which contained few-layers graphene oxide suspended in water, was poured out and the remaining precipitate (GO with more layers) was mixed again in Milli-Q water and then sonicated for 1 hour to break them into layers. The resulting suspension was allowed to stand again for 24 hours in order to precipitate. This process of re-suspension, sonication and precipitation was repeated for each precipitate until almost no precipitate was seen.
The next step in the synthesis was dialysis of the resulting few-layer GO colloid. This was achieved as follows. The dialysis membrane was soaked in Milli-Q water for ½ hour to remove any impurities. It was then washed with distilled water and one of its ends was securely clamped to ensure that no liquid could escape when filled. About 75ml of the GO colloid was filled into the membrane from the open end and any bubbles formed at the surface of the liquid were removed by pressing the membrane together and smoothing the area between the liquid surface and the open end of the membrane with the fingers. The open end was securely closed so that no liquid could leave the membrane, and was then completely submerged into a large beaker filled with Milli-Q water (about 2500ml), being agitated with a magnetic stirrer. The dialysis was done for 24 hours with the water being changed once during this period. Dialysis continued for the entire volume of the GO colloid, each time only cleaning about 75ml and using the same membrane. During this period, the batch to be dialyzed remained stirring in a beaker, while the batch that was already cleaned was poured into plastic containers (about 100ml) and placed in the freezer.
The containers of the frozen dialyzed GO colloid were covered with tissue paper, which was secured to the container with tape, and placed into a freeze dryer, where they were vacuum dried. They were removed from the dryer when the solid frozen mass and any residual water was no longer present in the container. The dried, brown, almost powder-like matter that remained was GO, which was then sealed in its container and stored in a desiccator.

2.1.2 Nano-Graphene Oxide Surface Activation

The synthesized GO was activated with carboxyl groups. This was carried out using chloroacetic acid and sodium hydroxide in the presence of water. 50mg synthesized GO was mixed in a flask, mounted on a retort stand, with 12.5ml Milli-Q water and sonicated for 45 minutes to ensure homogeneity. 37.5ml Milli-Q water was added to 2.5g NaOH pellets (Panreac 131687, M=40.00, ≥98.0% purity) and mixed with a magnetic stirrer until homogenized, then added to the GO mixture after sonication, but still being magnetically stirred. 2.5g $ClCH_2COOH$ (Sigma Aldrich 40293, ACS Reagent ≥99%) was then added to the GO mixture and stirred until homogenized. The flask with the new mixture was put to sonicate for 3 hours, changing the water in the ultrasonic bath if it becomes too hot.
The pH of the Milli-Q water was measured using a pH tester placed into the medium. The tester was then washed and placed in the GO mixture to determine its pH. A small glass Pasteur pipette was then

used to slowly administer drops of HCl to the GO mixture, checking its pH after every drop. When the pH of the GO mixture was very close to that of the Milli-Q water, no more HCl was added.

The resulting neutralized mixture was poured into four plastic sample holders, to be used in the centrifuge, each filled to about 40ml. The sample holders with the liquids were weighed and Milli-Q water added until the mass of all were roughly the same. They were then placed in the centrifuge on opposite sides and set at 10000rpm, acceleration at 9, deceleration at 6, for 10 minutes. At the end of the cycle the clear liquid was decanted from the holder leaving the precipitate and any liquid containing precipitate. This was again suspended with Milli-Q water, and the process of weighing and centrifuging repeated two more times under the same conditions.

After the last centrifugation, Milli-Q water was added to the resulting precipitate and put to freeze. Once frozen, the sample holders were covered with tissue paper fastened to the container with tape, and placed in the freeze dryer. The samples were removed once dried, leaving a dark brown to black, feather-light, powder.

Scanning electron microscopy (SEM) was done on the sample to determine the purity of the sample. When salts were found to be present, extra washing was done via centrifuging until no salts were seen on SEM. Fourier Transform Infrared (FTIR) and Dynamic Light Scattering (DLS) were also used to characterize the GO, providing evidence of its content and size.

2.2. Dry Functionalization

2.2.1 Atomic Layer Deposition (ALD) Reactor

The ALD apparatus used is a viscous flow reactor at the Ceramics and Materials Department at the Universidade de Aveiro. It was constructed in-house with stainless steel pipes and tubing components. The reactor flow tube has a length of 55cm and an inside diameter of 50mm. A schematic of the reactor is shown in Figure 9 and its images are shown in Figure 10.

Depositions are carried out in the reactor under a rough vacuum environment. A one-stage rotary vane pump is used (Vacuubrand, RE 2.5), recognizing a baseline pressure of approximately 2.5mbar during reactions.

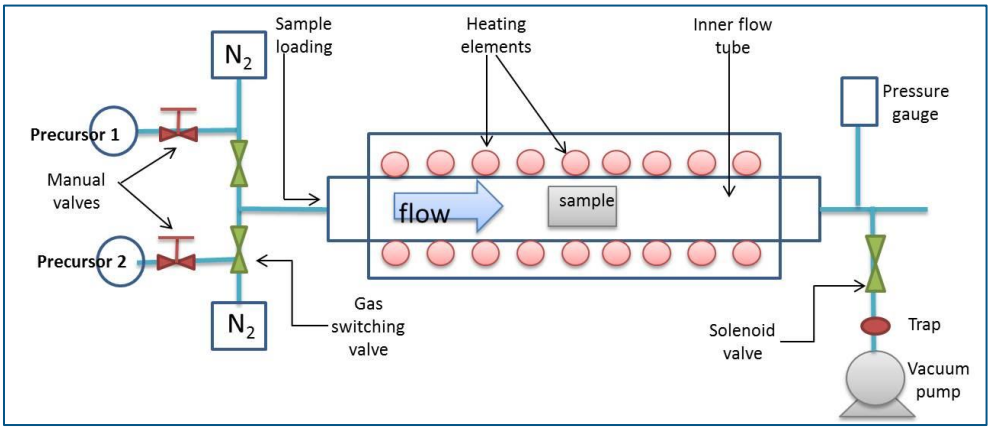

Figure 9: Schematic of ALD reactor used in this work.

The furnace tube is externally heated so that the loaded samples are heated by radiation and convection from the walls of the inner tube. The temperature of the furnace is electronically controlled. A control panel exists on the furnace so that the temperatures can be set. This is equipped with 3 channels of control corresponding to three thermocouples; 2 positioned closer to either end of the inner tube and one at the centre. The furnace also has a split configuration, allowing the inner flow tube and heating elements to be exposed when the furnace casing is opened (Figure 10), allowing for easier removal of the tube and inspection of the heating element.

Nitrogen gas (Air Liquide, Alphagaz 1; 99.999%) is used as a carrier gas for carrying the precursors to the flow tube, and for pulling the precursor, unreacted precursor and by products of the reaction through it. N_2 flows from the reactant lines through the inner flow tube and into the exhaust vacuum pump. The optimal flow rate of N_2 is 100ml/min. N_2 is sufficiently stable preventing reaction with other gases under vacuum. A trap, comprising an alumina filter, is connected before the vacuum pump with the purpose of capturing acid, water and particles which have passed through the flow tube.

The reactant lines connect the flow of nitrogen gas and precursors, directing them into the furnace. Pneumatic valves are placed just after the point where the reactant lines connect to the precursor canisters. These valves are opened with the pressure of the nitrogen gas, which is used as a carrier gas for the precursors. Manual valves are also placed on the lines connecting the precursor canisters in order to prevent precursor from entering the reactor when no reaction is occurring, but operates only for purging, and requiring only N_2.

Figure 10: Images of the ALD apparatus used for deposition; front view of the furnace with control panel (left), split configuration allows the furnace casing to be opened, showing the inner flow tube and heating element (right).

The inner flow tube spans a little beyond the area of the furnace casing. The temperature of these areas at the entrance and exit of the furnace can be controlled electronically, with input of the desired set points on the software used for programming the deposition. In addition, the temperature of the canisters housing the precursors can also be set in the same way. Heating of the lines and the tube facilitates the flow of precursors, preventing or minimizing accumulation in the lines and tube. Heating of the canisters enables an increase in vapour pressure of the precursor so that it may flow through the lines and into the tube.

As previously mentioned, deposition onto substrates placed in the chamber is set and controlled electronically by a software program on the computer. Temperature values are set to control the lines, exit and entrance of the tube, and the precursor canisters. Times are set for the duration of opening of the precursor valves, the residence time of the precursor in the inner flow tube and the purging time when only the N_2 flows, entraining unreacted precursor and by-products of the reaction, removing them from the furnace. The number of cycles for deposition can also be controlled, as well as successive purging cycles for cleaning the entire reactor before and after deposition. This includes the percentage of N_2 used and the times for opening of the valves to clean them.

There are two modes of operation of the reactor for deposition; continuous mode and exposed mode. The depositions in this research are carried out in exposed mode. A solenoid valve positioned after exiting the tube is important to this mode (Figure 9). In exposed mode this valve closes so that the interchanging precursors are kept in the inner flow tube, where the sample is positioned, for the duration of their respective residence times. This allows the precursors to interact with the sample, the sufficiency of which is determined by the duration and the nature of the precursor and sample, but the opportunity for interaction is increased in this mode. Once the pre-set and predetermined residence

time has elapsed, the solenoid valve opens and the precursor flows though, usually followed by N_2 for purging until the other precursor valve opens.
Monitoring the deposition cycle steps of purging-precursor A-purging-precursor B is done by pressure changes in the tube. A surge in vapour pressure is seen when precursors are pulsed into the furnace's inner tube and decrease when they exit and is maintained here throughout purging. Pressure changes are measured by an Edwards Active Pirani gauge, placed just after the end of the inner tube, before the solenoid valve (Figure 9), with the capability to measure pressure in the range from atmosphere to 10^{-3}mbar.

2.2.2 Dry Functionalization of GO Films via Vaporization-Condensation

This test involved the exposure of thin films of activated GO to amine-terminated polyethylene glycol (PEG) in the ALD reactor. GO was made into films for determination of optimized conditions for PEG attachment to its activated surface. The films are easier to handle than the powder and require the use of a smaller amount of sample per deposition.

Film Preparation

GO suspension was used to create thin films onto glass substrates. Glass substrates were cut into pieces of about $1cm^2$ and cleaned via sonication in acetone, ethanol and Milli-Q water, each for 10 minutes, after which they were dried in an oven at 200^oC overnight.
GO films were then prepared onto these substrates by drop casting. The synthesized activated GO suspension of concentration 1.8mg/ml, was dropped onto the substrates to cover a specific area and then allowed to dry in an oven at 80^oC for 15-20 minutes, until they were still viscous, not completely dried. They were subsequently air dried for about 20 minutes, forming a continuous film on the substrate.
In the cases where, after evaporation in the oven, it was noticed that the GO pulled away from the substrate, covering a smaller area than that desired, additional GO was dropped onto the surface and the procedure repeated. The drying times in these instances were at the lower end of the range stated above and at times even lower because of the higher temperature of the substrate when the drops were again administered.

Polymer Preparation

Amine-terminated PEG (452572-5G Aldrich – Poly (ethylene glycol) bis(3-aminopropyl) terminated, Mn 1500) in pellet form was used as the precursor. 0.5g of the precursor was mixed with 20ml Milli-Q for 30 minutes. It was then poured into a stainless steel precursor canister, which had been cleaned with ethanol and dried in an oven at 120^oC for 5 minutes prior to filling. The canister was then attached to the ALD reactor.

Deposition

The prepared substrates were placed in a ceramic sample holder. The vacuum on the ALD reactor was turned on and allowed to run for an hour. The temperature of the furnace was set to 80^{o}C, using the control on the furnace, and setting the temperature of the sample during deposition. The temperatures were then set on the software program such that that at the portion of the flow tube entering and exiting the furnace, the lines to the vacuum pump and the precursor canister were 100^{o}C, 100^{o}C, 100^{o}C and 85^{o}C, respectively.

The parameters were then set for purging with N_2; open time of the valves for 2s, residence time of 0.1s and purging time of 5s. Purging was carried out for 1000 cycles, after which the chamber was opened and the sample placed inside, at the centre of the furnace. Subsequent to this, purging was carried out in vacuum for 20 cycles, followed by the addition of N_2 for a further 20 cycles. The deposition parameters were then set; a valve opening time of 1s, residence time of 2s and a purging time of 120s, for 172 cycles, approximately 7 hours. On the start of the deposition cycle the precursor manual valve was opened.

The samples were removed after deposition, by first purging for about 20 cycles and subsequently stopping the vacuum before opening the flow tube to retrieve the sample. Characterization techniques were then performed on the films.

This procedure was repeated for different samples at different temperatures; 90^{o}C, 100^{o}C, 120^{o}C and 130^{o}C.

2.2.3 Dry Functionalization of GO Powder via Vaporization-Condensation

Functionalization of GO particles with PEG was carried out based on the results from functionalization of GO films.

Polymer Preparation

Amine –terminated PEG (Aldrich 14501-1G – poly(ethylene glycol) bis (amine), M_w 2000) was used as the precursor for deposition in the reactor. 0.5g of precursor in pellet form was mixed with 40ml Milli-Q water and mixed for 30 minutes. This solution was poured into a stainless steel canister, which had been cleaned with ethanol and dried in an oven at 120^{o}C for 5 minutes prior to filling. The filled canister was then attached to the reactor.

Deposition

The ALD reactor was turned on and the vacuum was allowed to run for about 1 hour, while the reactor stabilized at the set temperature of 90^{o}C. The temperatures were then set on the software program such that that at the portion of the flow tube entering and exiting the furnace, the lines to the vacuum pump and the precursor canister were 100^{o}C, 100^{o}C, 100^{o}C and 85^{o}C, respectively.

The parameters were then set for purging with N_2; open time of the precursor valve for 2s, residence time for 0.1s and purging time for 5s. Purging was carried out for 1000 cycles. 26mg of activated GO powder was placed in the ceramic sample holder, and a metal grid used to cover it, in order to contain the powder. The vacuum was stopped, the flow tube was opened and the sample in the holder placed at the centre of the tube. Once the tube was closed purging was set again and carried out in vacuum for 20 cycles, followed by the addition of N_2 for a further 20 cycles.
The deposition parameters were then set; a precursor valve opening time of 1s, residence time of 2s and a purging time of 120s, for 172 cycles, approximately 7 hours. On the start of the deposition cycle the precursor manual valve was opened.
The samples were removed after deposition, by first purging for about 10 cycles and subsequently stopping the vacuum before opening the flow tube to retrieve the sample. Characterization techniques were then performed on powder.

2.2.4 Dry Functionalization of GO Powder via MLD

In this deposition aluminium was used as an intermediary for attaching the carboxyl groups of the GO surface to ethylene glycol (EG) monomer.

Precursor Preparation

Ethylene glycol (EG) precursor (03760 Fluka ≥98.0%), already in solution with water, was poured into a cleaned stainless steel canister of the ALD reactor, until about ¾ full (35ml), then screwed into place. Trimethylaluminium (TMA) (257222 Aldrich 97%) was used as a second precursor. It was poured into another canister, filled to about 35ml, and screwed into place on the reactor.

Deposition

The ALD reactor was turned on and the vacuum was allowed to run for about 1 hour, while the reactor stabilized at the set temperature of 90^{o}C. The temperatures were then set on the software program such that that at the portion of the flow tube entering and exiting the furnace, the lines to the vacuum pump and the precursor canister were 100^{o}C, 100^{o}C, 100^{o}C and 85^{o}C, respectively.
The parameters were then set for purging with N_2; open time of the precursor valve for 2s, residence time for 0.1s and purging time for 5s. Purging was carried out for 1000 cycles. 20mg of activated GO powder was placed in the ceramic sample holder, and a metal grid used to cover it in order to contain the powder. To put the sample into the inner flow tube, the vacuum was stopped, the flow tube was opened and the sample in the holder placed at the centre of the tube. Once the tube was closed purging was set again and carried out in vacuum for 20 cycles, followed by the addition of N_2 for a further 20 cycles.
The deposition parameters were then set for TMA (precursor A); a precursor valve opening time of 0.5s, residence time of 1s and a purging time of 60s, for 20 cycles, about 20 minutes. The EG (precursor B) parameters were then set; a precursor valve opening time of 0.5s, residence time of 2s and a purging

time of 120s, for 172 cycles, about 6 hours. On the start of each precursor deposition cycle the respective precursor manual valve was opened.
The samples were removed after deposition, by first purging for about 10 cycles and subsequently stopping the vacuum before opening the flow tube to retrieve the sample. Characterization techniques were then performed on powder.

2.2.5 Check for Covalent Bonding

After deposition, GO films and powder were washed with the aim of removing any polymer or precursor adsorbed to the surface but non-covalently linked.
This was performed as follows; an amount of the sample material, sufficient for characterizing via the different techniques, was put into a small plastic tube and manually agitated in Milli-Q for about 2 minutes. The particles or pieces of film were allowed to settle and the excess water removed either by pouring or using a pipette. Water was again added to the GO and the procedure repeated. A smaller amount of water was added and the tube was placed in a freezer, and its contents dried via freeze drying.

2.3. Characterization Techniques

The following techniques were performed on the synthesized and functionalized material for determination of their respective characteristics, and for establishing a basis for comparison.

2.3.1 Dynamic Light Scattering

To determine the particle size of the synthesized GO, dynamic light scattering (DLS) was performed using a Malvern Zetasizer system. The zeta potential was also measured to determine changes in the potential (mV) of the nanoparticle surface before and after deposition attempts in order to verify the occurrence of surface functionalization.

2.3.2 Fourier Transform Infrared Spectroscopy

Synthesized GO

Fourier Transform Infrared Spectroscopy (FTIR) was carried out to determine the chemical compounds and bonding groups comprising the material. It was performed on a sample of the graphite used as the starting material in the synthesis of GO, on a sample of the synthesized GO before activation and on the synthesized GO after activation with carboxyl groups. The spectra were registered using Brucker Tensor 27 equipment, 256 scans in the range 400-4000cm^{-1}, with a resolution of 4cm^{-1}, and performed on KBr pellets in transmission mode.

PEGylated GO Films and Powder

FTIR was carried out on samples of the initial GO film and those after deposition with amine-terminated PEG in the reactor. It was also performed on the glass substrate. The spectra for the films were carried out using Brucker Tensor 27 equipment, 256 scans in the range 400-4000cm^{-1}, with a resolution of 4cm^{-1}, in FTIR-ATR (Attenuated Total Reflectance) mode.
GO powders after deposition and after washing were analysed using Brucker Tensor 27 equipment, 256 scans in the range 400-4000cm^{-1}, with a resolution of 4cm^{-1}, on KBr pellets in transmission mode. Washed GO films were also performed in this way.

2.3.3 Scanning Electron Microscopy

Scanning electron micrographs were obtained to characterize the morphology of the samples. This analysis was performed on synthesis samples; graphite starting material, GO before activation with carboxyl groups and activated GO. Micrographs were also obtained for the initial GO films and those after deposition and washing. GO powder samples before and after washing were also observed. SEM was performed on Hitachi SU 70.

2.3.4 Energy Dispersive Spectroscopy

Energy Dispersive Spectroscopy, EDS, measurements were carried out on a Bruker Nano GmbH system using an XFlash 5010 detector, to determine the elemental composition of the sample. This was obtained for synthesized activated GO and for GO powder functionalized via MLD.

2.3.5 Thermogravimetric Analysis

Thermogravimetric Analysis (TGA) was used to verify the presence and relative amounts of PEG or TMA-EG on the GO samples by measuring their thermal stability. NETZSCH STA 449F3 TGA instrument was used, and the procedure performed in an oxygen environment from 30^{o}C to 1060^{o}C at a rate of 5^{o}C/min. TGA was performed on GO powder samples after deposition with PEG, and TMA and EG.

2.3.6 Differential Scanning Calorimetry

Differential Scanning Calorimetry (DSC) was also performed using the TGA instrument, and on the same samples. It was carried out to confirm the presence of the polymer on the powder, by determining the temperatures at which any thermal reactions in the sample may occur.

CHAPTER 3 RESULTS AND DISCUSSION

3.1 Synthesis of Surface Activated Nano-Graphene Oxide

The modified Hummers' method resulted in the synthesis of GO with surface functional groups. The starting graphite is described by a double bonded carbon skeletal structure with the presence of adsorbed water and possibly few other functional groups, evidenced by its FTIR transmitted peaks at 1631cm^{-1} showing C=C vibrations[38,39], at 3442cm^{-1} corresponding to O-H stretching[38,39]and one at 1384cm^{-1} corresponding to C-OH stretching[39], shown in Figure 11. The oxidation of graphite was more than likely carried out by the formation of dimanganese heptoxide, Mn_2O_7, resulting from the reaction between potassium permanganate and sulphuric acid, with the inherent localized defects of the graphite's π structure acting as points of proliferation for oxidation[6].

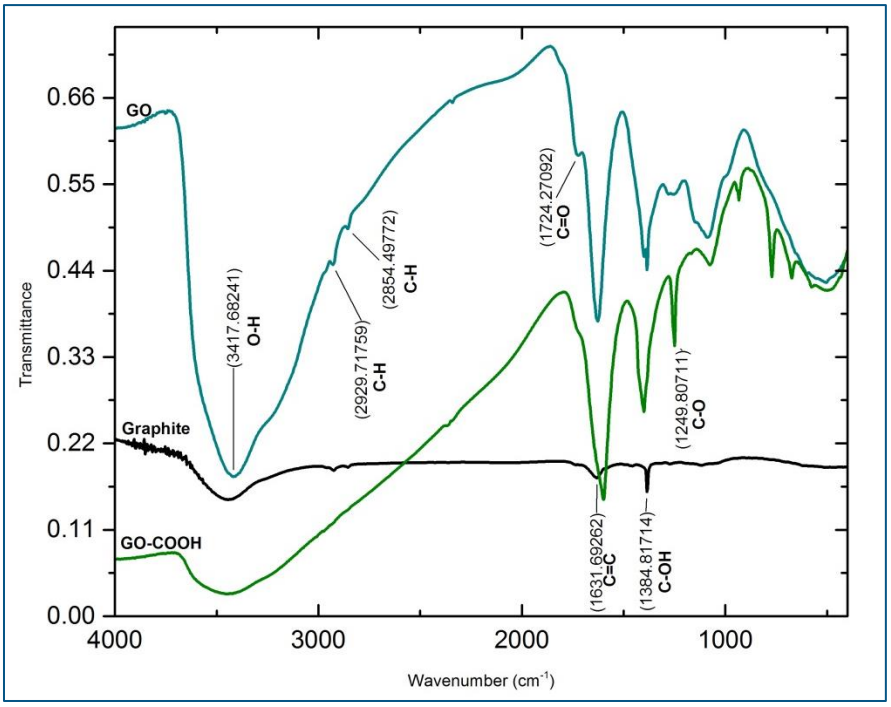

Figure 11: Measured FTIR spectra of graphite, non-activated GO and GO activated with carboxyl groups.

The resulting non-activated GO FTIR spectrum shows O-H stretching, C=C vibrations and C-O stretching transmittance, like with graphite, but appearing more pronounced than those present in the graphite spectrum, suggesting an increase in O-H groups and C-O bonding, due to oxidation of graphite. In addition, peaks at 2927cm^{-1} and at 2854cm^{-1} correspond to asymmetric and symmetric vibrations of C-H groups[40], and those at 1724cm^{-1} and 1087cm^{-1} to C=O stretching of carboxyl functional groups and C-O stretching vibrations, respectively[9,40,41]. Non-activated graphene oxide is described by carbon bonded in a hexagonal lattice with interplanar spacing larger than that of graphite or sheets of C=C, due to the intercalation of oxygen moieties. In addition, it possesses functional groups due to the synthesis

process, having hydroxyl and epoxy groups on its basal planes and carboxyl and carbonyl groups on the periphery[6]; hence an increase in the O-H peak, as well as the presence of C-O and C=O vibrations. A closer look at this measured GO spectrum with its reference is shown in Figure 12.

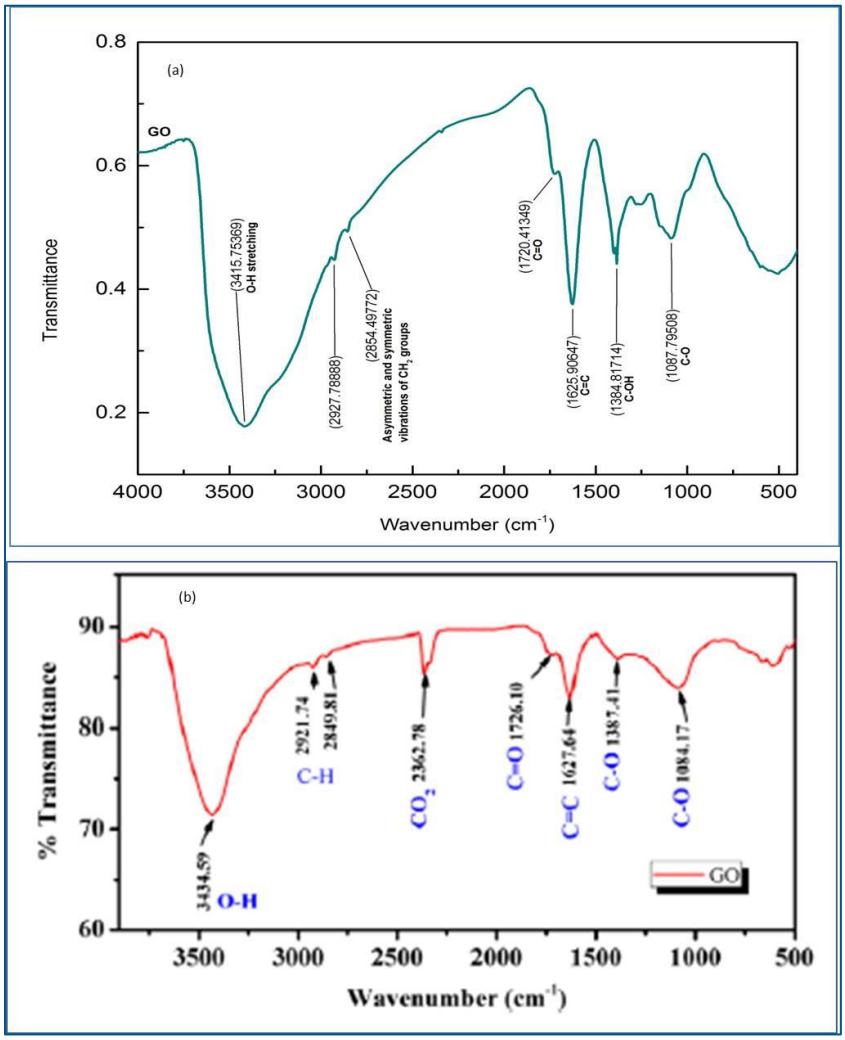

Figure 12: (a) Measured FTIR for non-activated GO; (b) Reference FTIR spectrum for non-activated GO[40]

The peaks at 2927cm^{-1} and at 2854cm^{-1} are identified in the spectra for both graphite and synthesized GO, and they account for C-H stretching vibrations[12,40]. Their presence can be explained by the structure of the starting graphite material comprising some aliphatic double bonds amidst its aromatic structure. During oxidation of graphite the Mn_2O_7 produced acts to oxidize these unsaturated aliphatic bonds, creating a variety of functional groups. This occurs because of the ability of dimanganese heptoxide to selectively oxidize unsaturated aliphatic double bonds over aromatic ones[6]. The graphite oxide intermediary exhibits its original unoxidized aromatic structure comprising sp^2 carbon but also aliphatic regions of sp^3 carbon and functional groups, both consequential of the oxidation process[42,43] and lent to

the eventual synthesized graphene oxide. It should be noted that the acidic activation of the GO surface is shown to remove the aliphatic component of the synthesized GO.

Finally, the activation of the surface functional groups of GO with chloroacetic acid and NaOH proved to be successful. The use of $ClCH_2COOH$ for GO activation in a strong basic environment should result in the activation of ester and epoxide groups, and convert hydroxyl groups to carboxylic ones[44]. The FTIR spectrum obtained for GO activated with carboxyl groups, GO-COOH, is also shown in Figure 11. Compared to that for non-activated GO, the presence of a well-defined peak at $1250cm^{-1}$ assigned to C-O stretching vibrations[9,41] of epoxy or ester groups, an increase in the peak around $1400cm^{-1}$ due to deformation vibrations of C-OH[40,41], possibly due to COOH groups, and the minimization of the O-H peak at $3417cm^{1}$, corroborate an increased number of carboxylic moieties on the basal planes and the periphery, and a loss of oxygen ones. The presence of the shoulder at $1724cm^{-1}$, attributed to C=O[40,44] of carboxyl groups, although not very pronounced in this image, also confirms surface activation.

In addition to identifying the major bonding groups of the synthesized activated GO, EDS analysis also provided its elemental composition (Figure 13). C and O are shown, authenticating the main components of the skeletal structure and functional groups of GO-COOH. Na and Si are also identified and are impurities resulting from the method of synthesis[45] and activation, Si possibly emerging from nanoparticle erosion of the glass beakers used for synthesizing, ageing and storing GO. The presence of these impurities would also impact the average size of GO measured in Figure 15 via DLS; some percentage of the higher diameters allocated to these impurities.

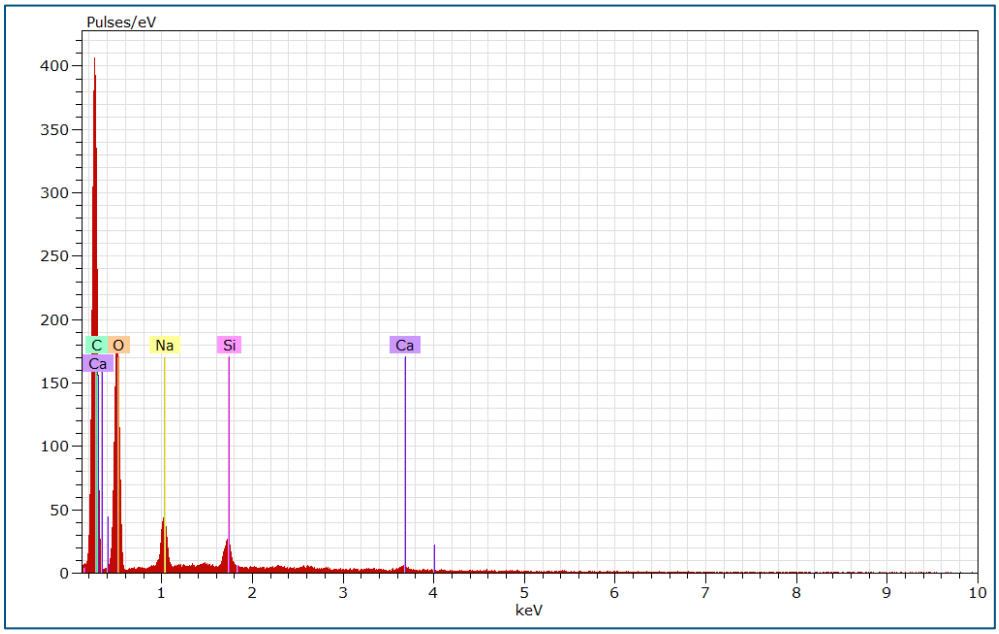

Figure 13: EDS elemental spectrum of GO-COOH

The synthesized nano-GO is shown in Figure 14. The suspension of graphene oxide activated with carboxyl groups (GO-COOH) is shown as an almost black suspension, while that of non-activated GO is brown. The difference in colour of the two suspensions has been explained by differences pH, owing to reduction effects upon activation of GO. The basic environment, under which GO-COOH is created,

changes the microstructure of GO, releasing local strain and partially restoring a reduced graphene structure via sheet conjugation[44]. This increased alkalinity lends to a darker suspension while increasing acidity would produce a lighter yellow/brown one[46]. pH differences also has implications for hydrophobicity and its corresponding agglomeration, acidic suspensions being known to portray these features, although the use of a strong base such as NaOH for GO surface activation will result in precipitation in aqueous media due to salt effects[46].

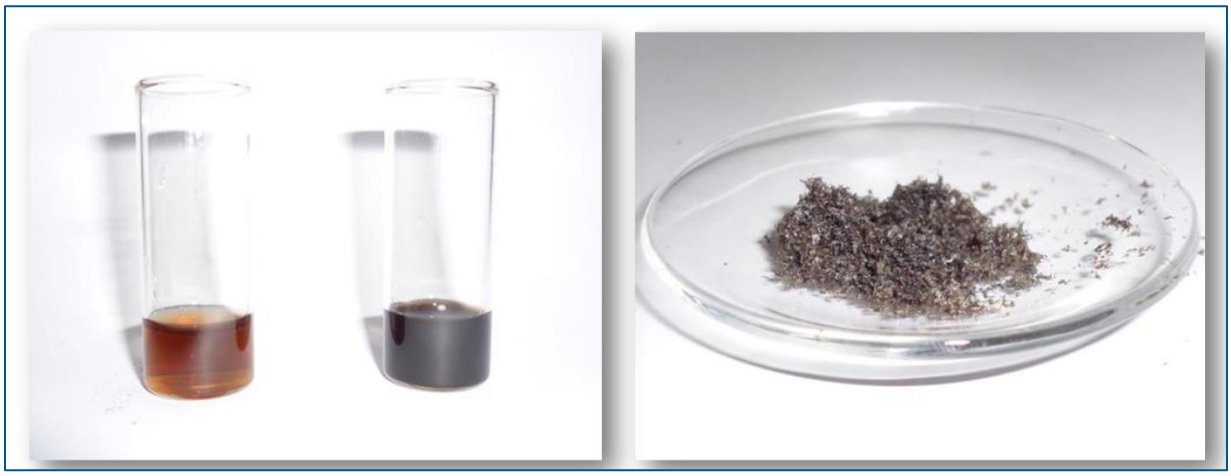

Figure 14: Images of synthesized nano-GO in Milli-Q water (left), the brown suspension is that of GO before activation with -COOH, and the black suspension is that after surface activation. Activated GO powder (right) is the result after freeze drying.

Dried, powder GO-COOH is also shown and can be described as a very light-weight material, full of electro-static energy, even more than that of non-activated GO, making it somewhat difficult to handle and resulting in loss of material when being transferred. The concentration of the GO-COOH solution was found to be 1.8mg/ml and the average main diameter of it particles was found to be 37.84nm, determined by dynamic light scattering (DLS). The measured DLS distribution is shown in Figure 15, indicating an estimated range of diameters between 24nm and 190nm with the highest frequency accounting for 29% of the tested sample.

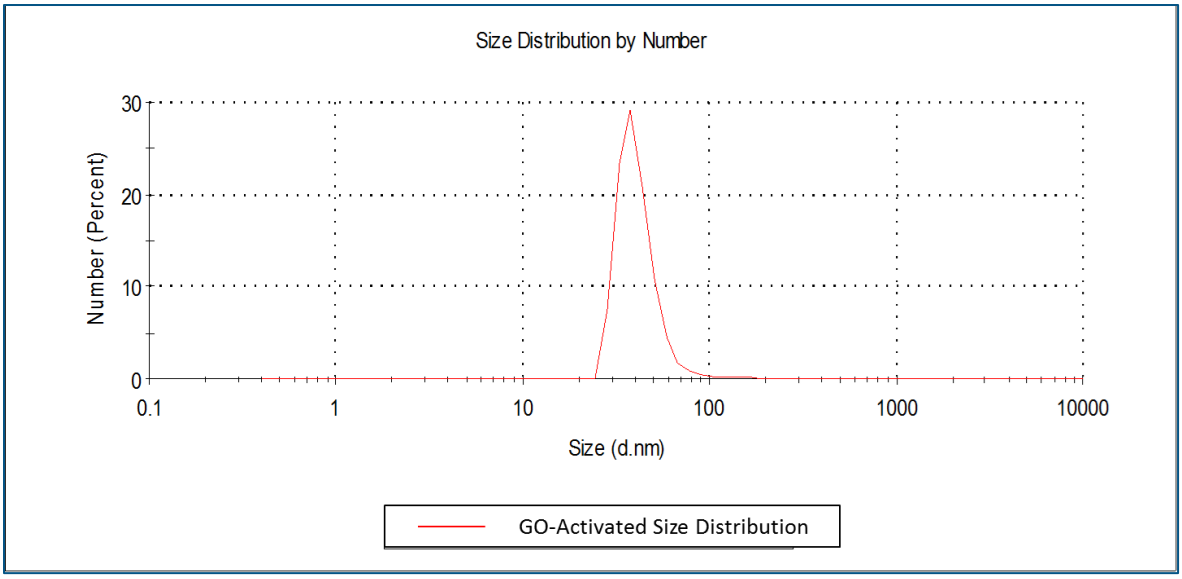

Figure 15: DLS histogram of one test measurement, showing the distribution of diameter sizes of the particles in a sample of synthesized, activated graphene oxide.

The SEM images for graphite and synthesized GO, non-activated and activated are shown in Figure 16. The plate-like, rigid structure of graphite is shown in (a) while (b) shows the structure of synthesized, non-activated GO, which typically recognizes larger spacing in between the layers due to the intercalation of functional groups giving it a more flake-like appearance compared to graphite. GO-COOH (c) is comparable to that of GO, showing flakes, possibly even smaller ones due to the activation process involving ultrasonication, which produces breakage of nanoparticles at their defect sites.

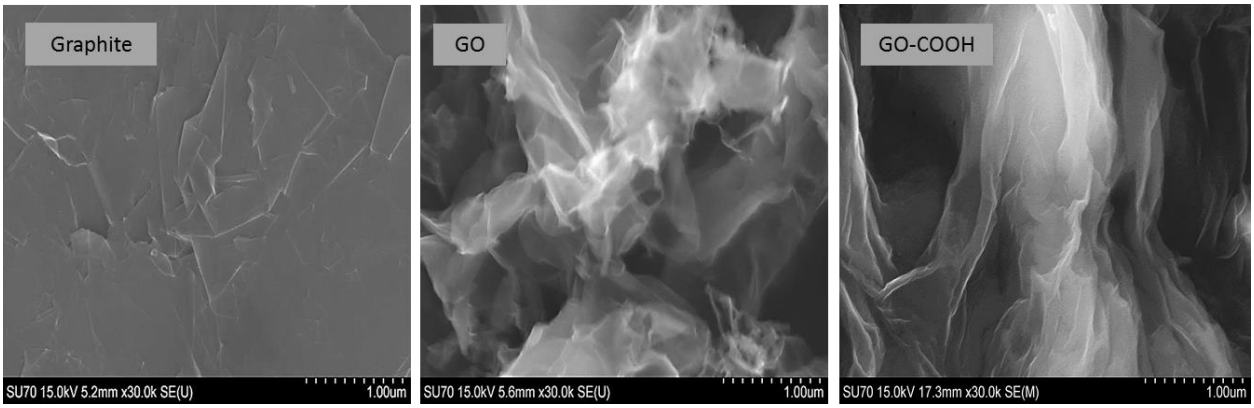

Figure 16: SEM images for the material in the progression of synthesized, activated GO; starting graphite material, synthesized GO and GO-COOH.

3.2 Dry Surface Functionalization in the ALD Reactor

3.2.1 Dry Functionalization of GO Films via Vaporization-Condensation of PEG

Deposition of PEG onto GO films on glass substrates was performed to control environmental parameters for PEGylation. The process of drop casting produced a film of GO-COOH onto the glass substrate, completely covering an area of the substrate, but not uniformly so, suggesting the presence of surface roughness. FTIR analysis of the film shows the presence of characteristic peaks of GO-COOH although being much smaller. The peaks at 1724cm^{-1}, 1593 cm^{-1} and 1382 cm^{-1} have already been identified in Section 3.1, as C=O stretching[40,44], C=C stretching of the GO skeletal structure and C-OH deformation vibrations[39–41], respectively. The peak at 1250cm^{-1} of C-O stretching[9,41] is not present in the GO film possibly suggesting the absence of ester or epoxy functional groups and emphasizing the overall smaller quantity of activation sites.

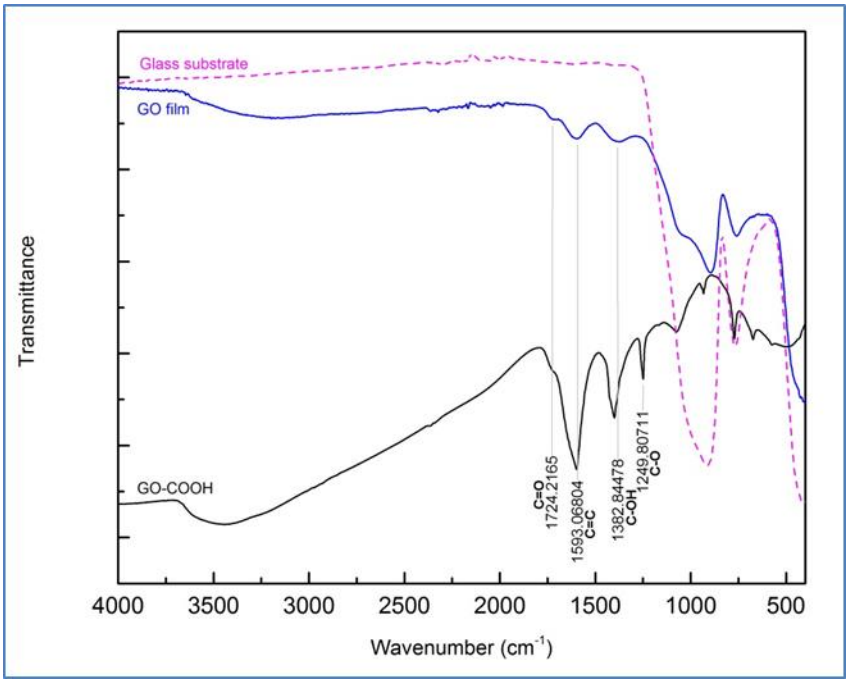

Figure 17: FTIR spectra comparing GO-COOH and GO films produced by drop casting (spectra have been shifted for clarity).

Discrepancies between the two spectra can firstly be explained by the use of different FTIR techniques. The measurement of the film was taken by FTIR-ATR rather than transmittance mode with KBr which was used to obtain the GO-COOH spectrum, the surface of the film therefore becomes important in

attaining a precise spectrum with low noise. The presence of bands as opposed to peaks, may suggest vagueness in measurements. Secondly, the hydrophilic nature of GO causes merging and stacking of its sheets on drying, thereby trapping gas molecules in between layers and creating defects in the microstructure when released. The layering of the GO-COOH sheets also suggests a change in the functional groups, as they must overcome their electrostatic repulsive forces to agglomerate.
It is also shown in Figure 17 that after around 1100cm^{-1} the spectrum for the GO film closely follows that of the glass substrate, demonstrating the contribution of the substrate to the FTIR spectrum.

The deposition of PEG onto the prepared GO films can be analysed by the chemical changes observed for the initial film, those after deposition and then after washing with Milli-Q water. Figure 18 shows the FTIR spectra for the films, for deposition at 90°C, and also that for the amine-terminated PEG precursor used. The chemical changes observed in the spectra of the films show the successful deposition of covalent PEG.
Characteristic peaks of the precursor powder, amine PEG, are seen at 2925cm^{-1} and 2854cm^{-1} for the CH_2 asymmetric and symmetric stretching of the aliphatic PEG structure[31,47,24], and also at 1630cm^{-1} for N-H bending[47] of the NH_2 amine termination of PEG. The peak centred at 3442cm^{-1} can be due to O-H stretching[48–50] of water, but may also be due to the N-H stretching[47] of the terminating amine groups.

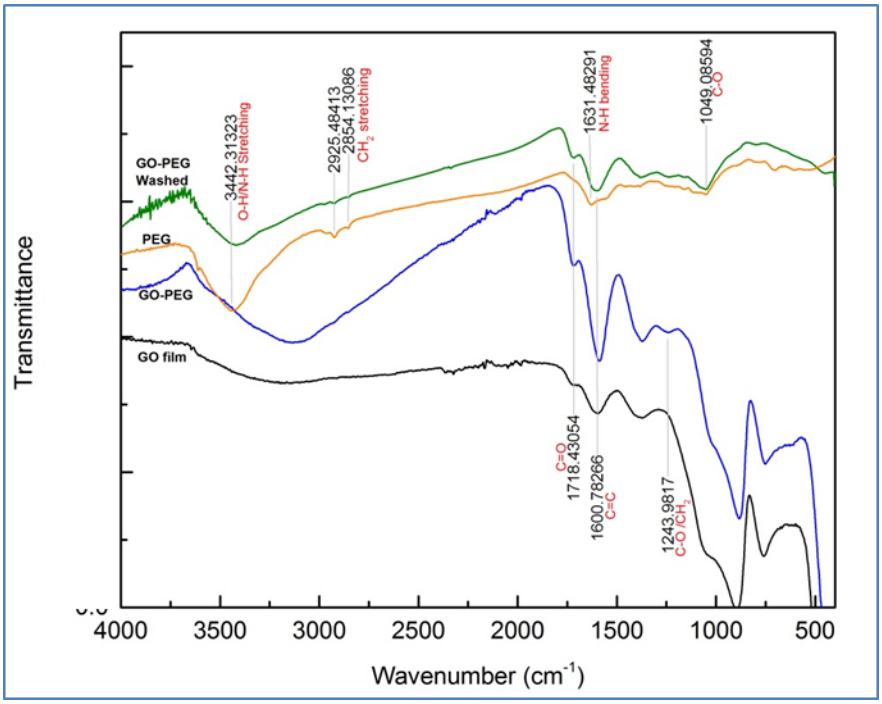

Figure 18: FTIR spectra comparing GO film before deposition, after deposition at 90°C, after washing, and that of the amine PEG precursor used.

A comparison of the initial GO film and that after deposition with amine-terminated PEG shows an increase in the peak at 1600cm^{-1}, corresponding to the stretching of double bonding carbon from C=C stretching of the skeletal benzene ring of the GO structure[44,49], but also identified as C=O stretching[24].

There is also a new peak around 1243cm^{-1}, ambiguously seen on amine PEG, but seen to be associated with CH_2 twisting[31], or C-O stretching of GO[9,41]. The intensification of the peak at 1718cm^{-1} is observed for GO samples after deposition and before washing, corresponding to C=O stretching of ester linkages[44,49]. Characteristic PEG peaks at 2925cm^{-1} and 2854cm^{-1}[31,47,24] are mildly visible on the GO-PEG spectrum.

In general, the peaks of GO-PEG after deposition and those after washing showed some shifting compared to the reference values identified. The measured spectrum after washing of GO-PEG in Milli-Q and freeze drying, to check for covalent bonding of PEG with GO, shows distinctly the presence of peaks at 2925cm^{-1} and 2854cm^{-1}, characteristic of the CH_2 asymmetric and symmetric stretching of PEG, although sometimes identified as one peak around 2878cm^{-1} [44,24,48–50]. This provides evidence that a covalent conjugation of PEG, these peaks representing its aliphatic structure[47].

Washing of the sample indicates covalent attachment since PEG is soluble in water and will be removed with it, if it is only adsorbed to the GO surface. The increased visibility of these peaks after washing, compared to the sample before washing, may be explained by the proliferation of a physical coating on the film, much more so than chemical bonding at the surface activation points, thereby diluting the transmission from these vibrations. Washing away the coating facilitates a better analysis of any surface functionalization that may have occurred in the reactor. It may also be due to the difference in obtaining the measurement, the GO-PEG sample being measured as a film, still attached to the glass substrate, using FTIR-ATR, and the GO-PEG washed sample measured as a powder in KBr in transmission FTIR, the effects of the latter being better for a nanocomposite particle. The transmittance of signals for these particular peaks should also be considered, being unmistakeably present in the PEG spectrum but comparatively small compared to other peaks. The presence of even smaller peaks after deposition and washing are expected since PEG will be attached only where the surface is activated, which is only at points of defects in the GO structure.

The washed sample also shows a peak around 1043cm^{-1} for C-O stretching, possibly also due to ester linkages[47], present also in amine PEG. This peak and that at 1600cm^{-1} could possibly be shifted peaks, as spectra for PEGylated GO identify amide-carbonyl bonding (NH-CO) at 1650cm^{-1}[44,51] and C-O at 1100cm-[124] as evidence of functionalization, together of with that of 2878cm^{-1}. It can be concluded from the FTIR spectra of Figure 18, that dry functionalization of GO with amine-terminated PEG was achieved via vaporization-condensation of PEG at 90^{o}C.

The temperature dependence of dry functionalization of GO by this method was analysed by comparing the chemical structure and morphology of each of the resulting samples. A comparison of the FTIR spectra for each of these samples, exposed to vapour PEG at 80^{o}C, 90^{o}C, 100^{o}C, 120^{o}C and 130^{o}C, before washing, is shown in Figure 19. The prominent peaks are those at 1224cm^{-1} and 1064cm^{-1} for C-O stretching[31,50], as well as that around 1577cm^{-1} of C=O[24,49], the reference spectrum being shown in Figure 20. It could also possibly be that some shifting may have occurred, as was earlier discussed, the measured peaks of 1064cm^{-1} and 1577cm^{-1} corresponding to C-O and NH-CO, respectively, usually characterized at 1100cm^{-1}[124] and 1650cm^{-1}[44,51], respectively. The remaining characteristic PEG peaks of 2925cm^{-1} and 2854cm^{-1}, previously identified in Figure 18, is vaguely shown in the spectra of GO-PEG at 80^{o}C, 90^{o}C and 100^{o}C, suggesting that these temperatures provide better conditions for deposition of vapour PEG.

In addition to this, there are other marked differences among the spectra obtained for PEG depositions at different temperatures. Firstly, there is the absence of the O-H band centred at 3130cm^{-1}, for the spectra of 120^{o}C and 130^{o}C. This is expected as the O-H here is most likely due to the presence of water adsorbed to the surface of the nanomaterial, which will be removed at these temperatures.

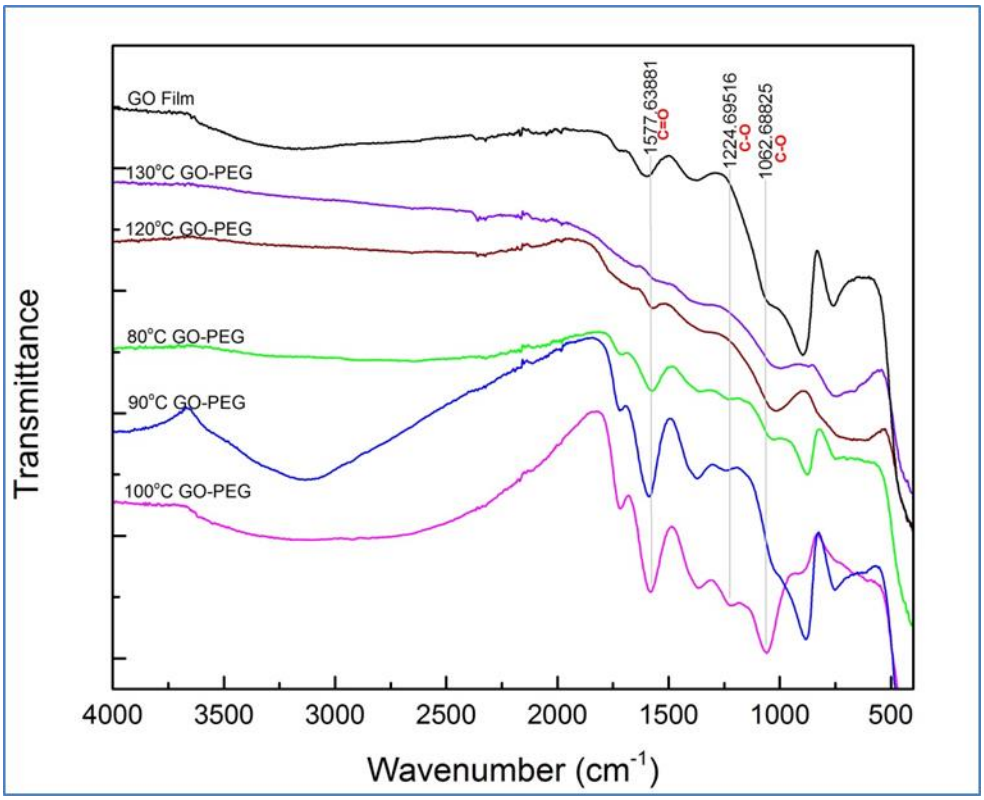

Figure 19: FTIR spectra of samples after deposition at all temperatures.

Secondly, the peaks identified for PEG in the spectra for temperatures 80^{o}C, 90^{o}C and 100^{o}C, are clearer than those of 120^{o}C and 130^{o}C, suggesting that deposition of the polymer is better achieved at lower temperatures. The loss of water from the surface of GO starts below 100^{o}C with further losses of CO, CO_2 and steam proliferating from the most labile functional groups of carboxyl activated GO[9] and PEG. These losses change the composition of GO leading to the absence of functional groups and subsequent bonding at the GO surface, thereby explaining the changes in the spectra for deposition at higher temperatures of 120^{o}C and 130^{o}C. Another explanation may be errors in measurement due to the GO film roughness, exacerbated by tearing of the film at these higher temperatures to release gases and steam from between the layers of GO.

The samples used to obtain the spectra of Figure 19 were washed to obtain those of Figure 20 (a). The spectra for all the temperatures were quite similar showing the identified characteristic peaks in accordance with the reference spectra[24] of Figure 20 (b), and confirming the covalent attachment of PEG. It is interesting to note that the CH_2 stretching peaks are not seen in the unwashed samples of 120^{o}C and 130^{o}C, but are undoubtedly present in the spectra of their washed samples. This could be the

result of measurement errors and the effect of particulate analysis in contrast to film analysis, the washed films being measured in transmission mode. It could also be the augmentation of the signal associated with these aliphatic bonds once non-covalently attached PEG is washed off.

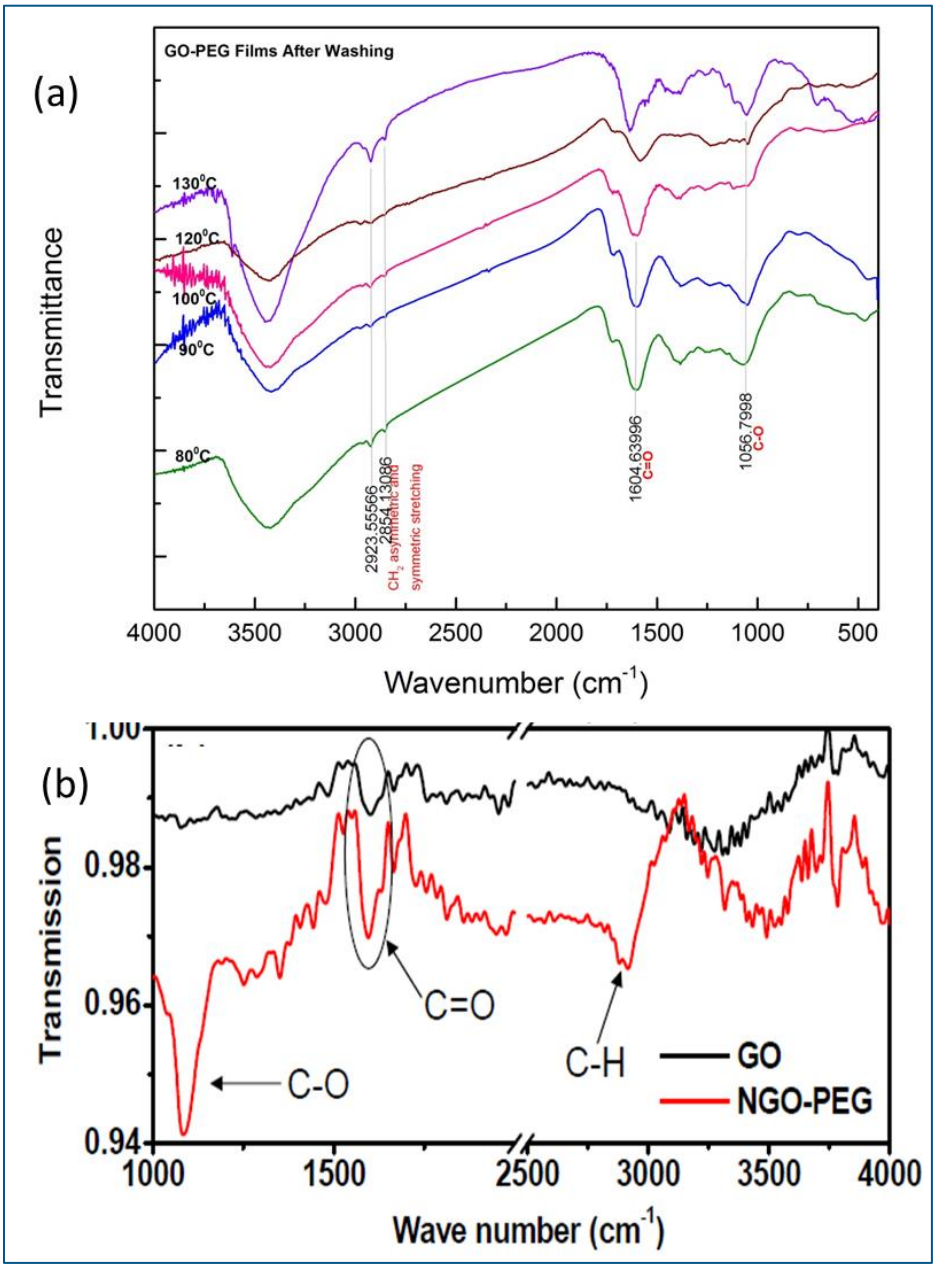

Figure 20: (a) Measured FTIR spectra of samples after washing; (b) reference spectra for GO functionalized with amine-terminated PEG[24] (note that the wavenumbers are descending in (a) and ascending in (b)).

The presence of the characteristic PEG peaks not only confirms dry functionalization of the GO but substantiates the parameters for achieving it; set times of 1s to open the precursor valve, 2s for residence of the vapour in the inner flow tube and 120s for purging, being adequate for reaction between the GO surface and PEG. Lower temperatures, between 80°C and 100°C, provide less ambiguity

in determining the chemical compounds comprising the resulting functionalized nanomaterial, suggesting that this vaporization-condensation approach is temperature dependent.

This result is not reiterated in the analysis of morphology by SEM images (Figure 21). GO-PEG at each temperature and after washing do not show marked differences among themselves, nor when compared to synthesized GO (Figure 21).

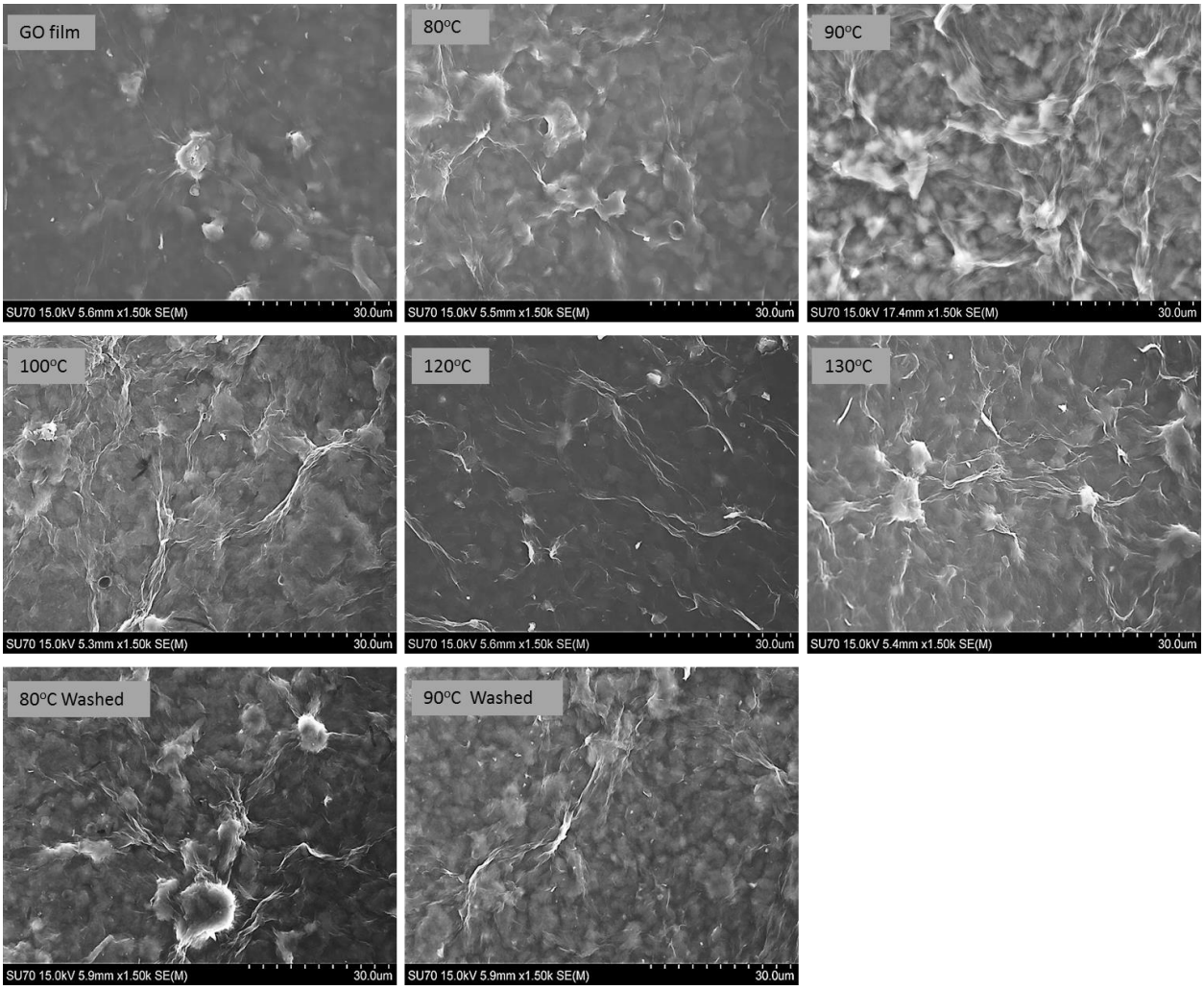

Figure 21: SEM images of GO film samples prior to deposition (GO film), after deposition of amine-terminated PEG (80°C to 130°C), and after washing with Milli-Q.

3.2.2 Dry Functionalization of GO Powder via Vaporization-Condensation of PEG

Based on the success of dry functionalization of GO films at lower temperatures, deposition of amine-terminated PEG was carried out on GO powder at 90°C. The success of this functionalization was important for the purpose of this work as the use of powders, rather than films, are more used in biomedical applications. It therefore delivers PEG to the synthesized GO-COOH material, without prior subjection to heating and drying for film formation.

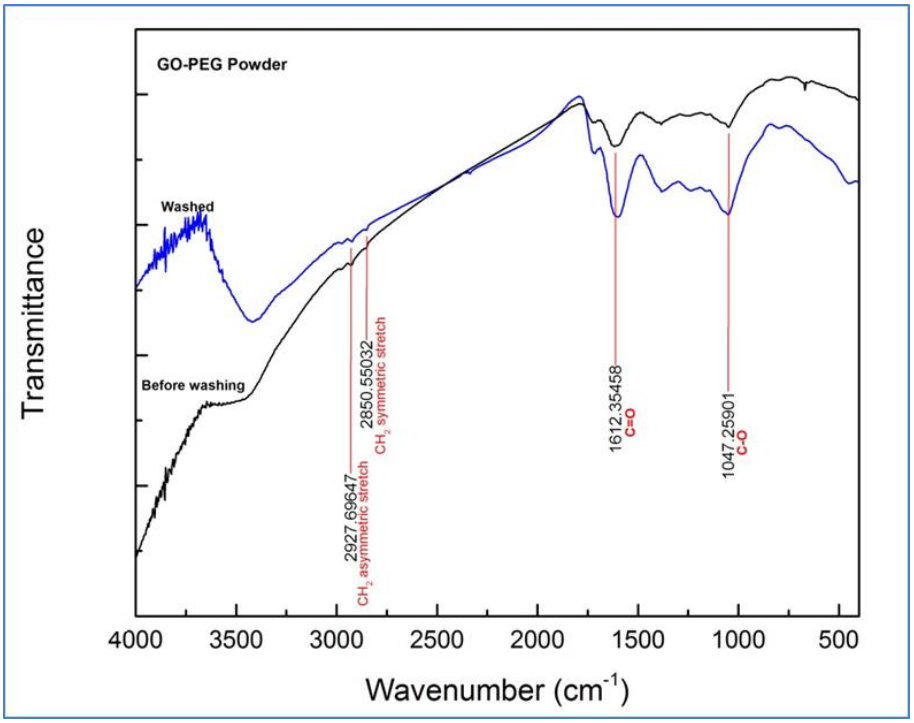

Figure 22: FTIR spectra of PEG functionalized GO powder

Analysis of the FTIR spectra for the GO powder after deposition and after washing (Figure 22) confirms the covalent bonding of PEG to the activated GO. Characteristic PEG transmittance peaks at 2928 cm^{-1} and 2850cm^{-1}[31,24,48,49] of PEG's aliphatic structure, C=O at 1612cm^{-1} possibly contributed from the amide bond between the NH_2 terminating PEG group and the COOH activated site of GO[44,51], and C-O at 1047cm^{-1}[24] also from the PEG repeating unit of CH_2CH_2O, signifies the conservation of the bonding group composition before and after washing. As with the GO films, the success of functionalization via the vaporization-condensation of PEG in the ALD reactor suggests that the set parameters were sufficient for the reaction.

Surface functionalization was also verified by the difference in the zeta potential between initial GO-COOH and the GO-PEG powder after washing. The zeta potential for initial GO-COOH was found to be

-41.8mV, while that of GO-PEG was -39.5mV, indicating that the GO surface after exposure to PEG was less negative (more positive) than that of surface activated GO. This is expected and can be explained by the surface reactions occurring between the carboxylated surface and PEG chains.

Figure 23 serves to demonstrate what ideally transpires in the ALD chamber when the carboxylated GO surface is exposed to amine-terminated (homobifunctionalized) PEG vapour. Carboxylation of the GO surface renders negatively charged hydroxyl groups, which attaches to the amine (NH_2) end group of PEG creating amide bonds and securing the polymer chain. The free end of the attached chain also ends in an NH_2 group, creating a surface that is more positive than that of GO-COOH. It would therefore be expected that after functionalization the zeta potential of the nanocomposite surface would become less negative that is, tending to positive, as was noticed in the measured values.

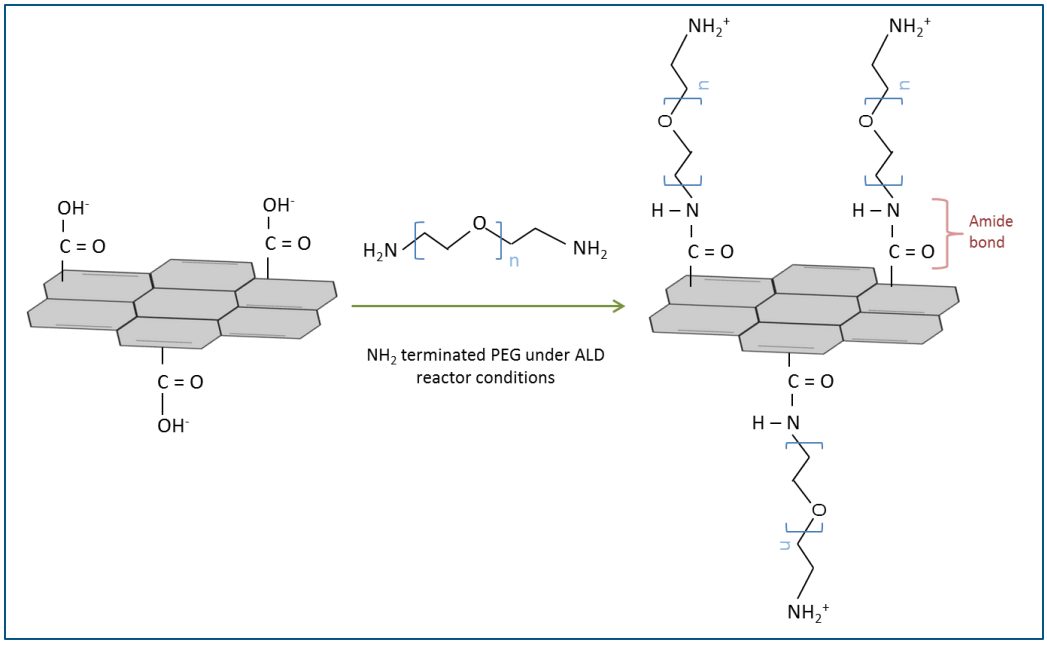

Figure 23: GO surface reaction between amine homobifunctionalized PEG and carboxyl groups.

It is pragmatic to consider that PEG may not necessarily interact with the carboxyl groups in the way proposed in Figure 23. It could occur that the both NH_2 groups of one PEG chain form amide bonds with two distinct surface groups, in so doing, eliminating the surface NH_2 groups and their associated charge. This will however preserve the expected outcome of the zeta potential to the extent that it should still be less negative than that of GO-COOH. It was identified that the prevalence of this conjugation is dependent on the distance between attachment sites of the activated surface and its deviation from the Flory radius, a parameter dependent on the length of the PEG chain[13]. A double reaction of a single PEG chain is supported when the site separation distance is greater than the Flory radius[13].

Thermal stability of the resulting nano-powder was investigated to further characterize it and quantify the amount of PEG deposited onto GO. GO-PEG powder was determined to be thermally stable below 152^{o}C in an oxygen environment, evidenced by the TGA curve of Figure 24(a). The nanocomposite sample shows an initial decrease in sample mass for temperatures under 100^{o}C due to the loss of

adsorbed water molecules on the sample[48]. This is followed by a further decrease, beginning around 152°C and continuing until around 196°C, signifying the start of GO decomposition, typically shown from 160°C to 230°C[48], on account of the release of CO, CO_2 and steam from the most labile functional groups[9]. The measured DSC (Figure 24(b)) however shows that this step may be mainly due to the loss of PEG chains which experiences its principal exothermic reaction between 175°C to 230°C.

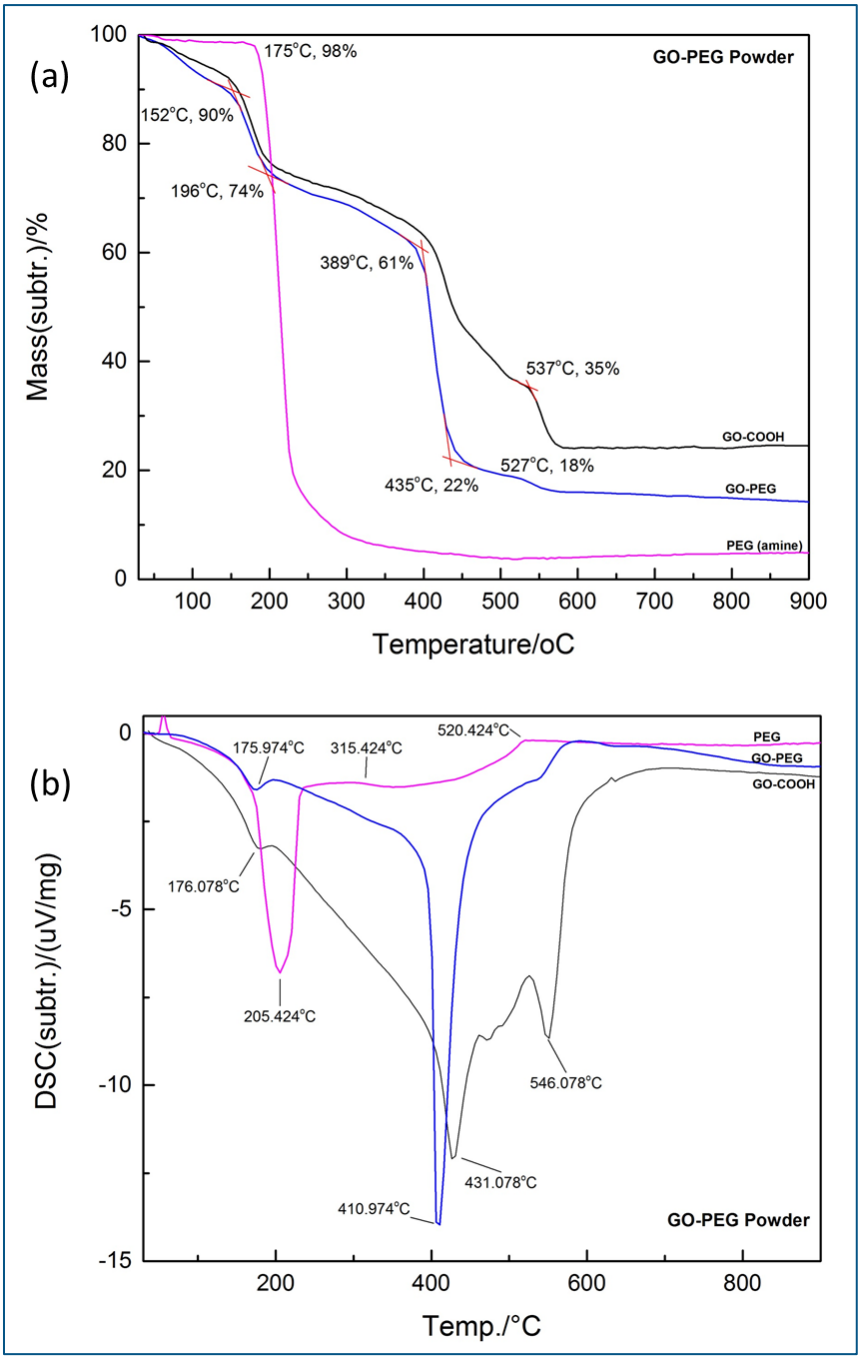

Figure 24: (a) measured TGA graph for GO-PEG powder; (b) measured DSC curve of GO-PEG powder.

The next deposition step, occurring from about 389^{o}C to 435^{o}C, is attributed to the thermal degradation of GO owing to the removal of its more stable oxygen functionalities[9], as well as that of PEG[52], shown by the similarity in shape to the PEG TG curve and the presence of an exothermic band on its DSC curve between 315^{o}C and 520^{o}C. A smaller decomposition curve occurring around 527^{o}C for the GO-PEG nanocomposite can be explained by the remaining GO, possibly residue of its skeletal carbon structure. It may however be expedient here to consider the impurities of Na, Si and Ca seen previously in the EDS of synthesized GO-COOH, which may to some extent attribute to this mass loss at higher temperatures.
Overall, the presence of PEG does not seem to significantly alter the thermal stability of GO. The TG curve of the nanocomposite follows that of GO, with PEG seeming to demonstrate its influence around 411^{o}C during the second decomposition step. The two main decomposition phases comprise mass loss of both GO and PEG making it difficult to determine the quantity of deposited PEG.

Morphological characterization of the GO-PEG nanocomposite powder by SEM demonstrated a similar structure to GO-COOH. SEM images of Figure 25 (a) and (b) showed GO-COOH at different magnifications, in comparison to (c) and (d) for GO-PEG.

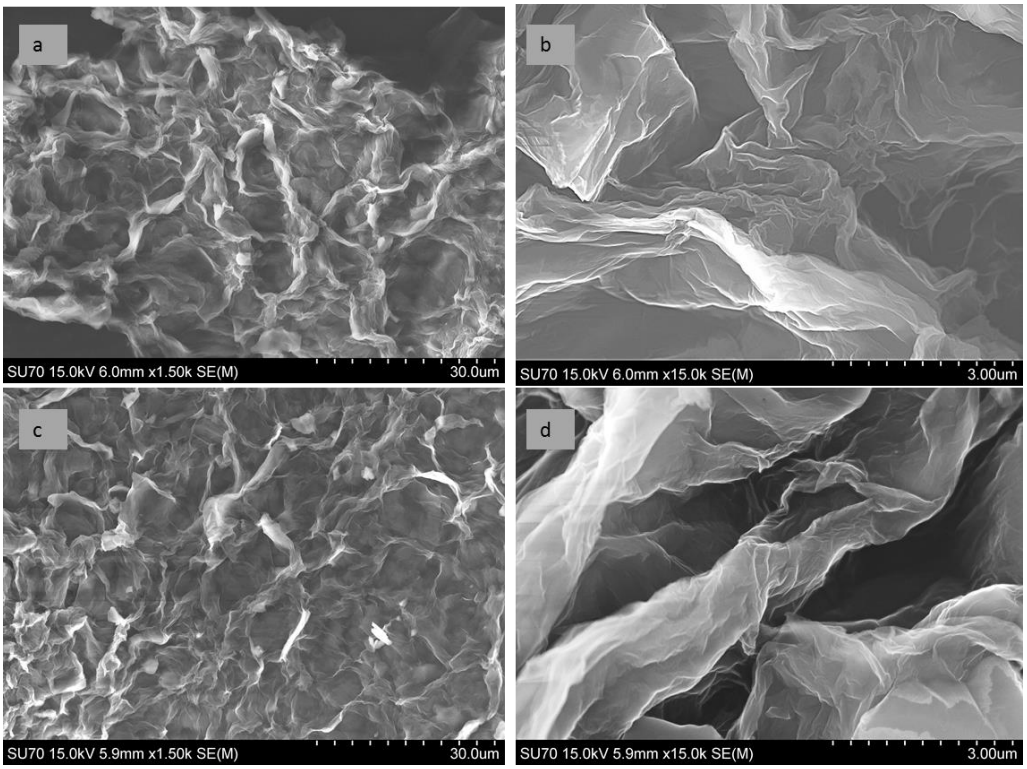

Figure 25: SEM images of the initial GO material (a) and (b), and the GO powder after PEG deposition (c) and (d).

3.2.3 Dry Functionalization of GO Powder via MLD.

The MLD approach for dry functionalization of GO-COOH powder was carried out with two precursors; trimethylaluminium (TMA) and ethylene glycol (EG). This was done as a platform for stabilizing the EG onto GO via active Al sites and providing a basis for molecular control for the future deposition of a polymer.

Surface functionalization of GO was successful, demonstrated by the presence of characteristic PEG peaks on the FTIR spectra for both washed and unwashed GO-TMA-EG nanocomposite (Figure 26). These spectra show few differences and display the characteristic PEG peaks at 2925cm^{-1} and 2852cm^{-1} [31,24,48,49], due to its aliphatic structure and those of C=O, characteristic of the amide bond, and C-O at 1612cm^{-1} [24,49] and 1062cm^{-1}[31,50], respectively. The spectrum of GO-PEG is also shown in Figure 26 for comparison.

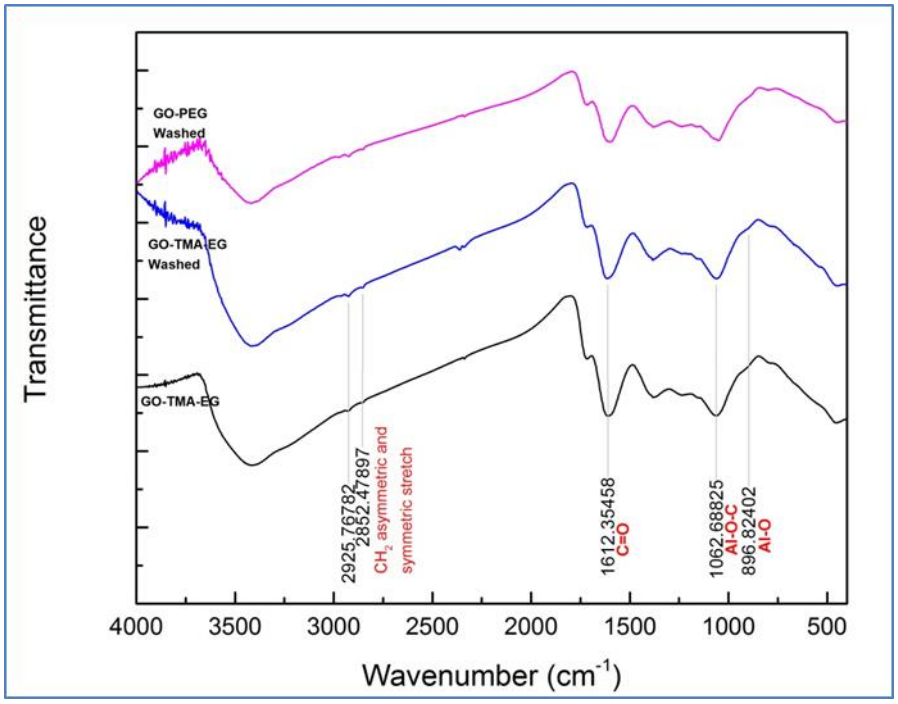

Figure 26: FTIR spectra of samples of GO powder after MLD with precursors TMA and EG, before and after washing, with that for GO-PEG also showed for comparison.

The presence of Al is however a bit more difficult to observe due to them being superimposed onto those of GO-PEG. Al-O stretching vibrations have however been identified around 905cm^{-1} after MLD was performed with the same precursors on an ALD grown Al_2O_3 surface[31]. A small shoulder around 896cm^{-1} present on the GO-TMA-EG samples could account for this bond but is inconclusive due to its very small size and presence in the washed GO film samples and GO-PEG powder samples.

Al-O-C bonds were characterized around 1100cm^{-1} for reduced GO-alumina composite powders[53]. This peak is present in all the samples of Figure 26, but could prove the presence of Al since the source of the C-O bond is inconclusive. If these groups are in fact present, they are the result of MLD. A schematic of

the MLD sequence and expected growth is shown in Figure 27 and reproduced from Dameron, et al, 2008[31]. Activated GO has on its surface OH groups from COOH. Exposure to TMA, $Al(CH_3)_3$, permits the positively charged Al ions to bond with the negatively charged surface groups, under vacuum conditions, and the resulting CH_4 gas is removed with N_2 purging. After the 20 cycles of TMA exposure, the surface of the GO powder should have been sufficiently coated with Al ions. Subsequent exposure to EG ($OHCH_2CH_2OH$), allows its OH groups to react with these surface ions thereby stabilizing the monomer and releasing its H ion to CH_4 gas which is removed by purging. The resulting hybrid could be likened to $AlOCH_2CH_2OH$, verifying the presence of Al-O-C groups.

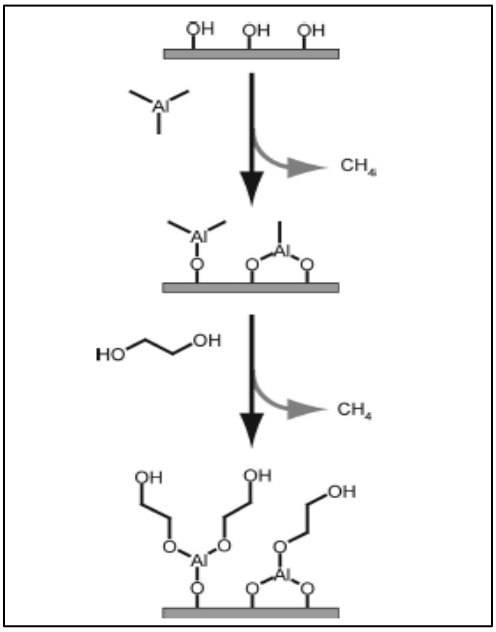

Figure 27: MLD sequence for TMA and EG precursors[31]

It should be noted that EG can also attach to the Al ions at either end[31] thereby removing OH groups from the resulting coating and preventing further attachment. The O-H peak of the FTIR spectra, around 3400cm^{-1} does show a slight increase from that of GO-PEG and this could be explained by the presence of OH groups at the end of the EG chain in the hybrid coating, or to the adsorption of water onto the surface of composite powder.

The ambiguity associated with Al-O bonding may be explained by these groups accounting for a very small amount of the total sample, having only been supplied during 20 cycles as opposed to 172 for EG. The dry functionalization of the GO powder via this method demonstrated greater consistency between the deposited and washed samples compared to deposition only with PEG. This is addition to the presence of characteristic EG peaks, suggests that the use of TMA did provide a site of attachment for EG.

The success of functionalization also attests to the sufficiency of the MLD parameters to bring about the proliferation of a hybrid structure. The parameters chosen were modified from those proven to be optimal for MLD by TMA and EG cycles to obtain alucone films[31]. It was therefore not especially necessary to have such long purging times as the same precursor was purged for successive cycles. The

purging phase is needed, even with the same precursor, to prevent unadsorbed reactant from being deposited on the walls of the reactor, thereby changing the pressure conditions inside the reactor. On this point, it is important to note the absences of CH_3 peaks on the FTIR spectra, which would have suggested the presence of TMA on GO, had they been present.

A zeta potential of -54mV was obtained for GO-TMA-EG compared to -41.8mV for GO-COOH. It is expected that for negatively charged hydroxyl groups of the bi-functionally terminating EG, as seen in Figure 27, a more negative zeta potential will result. It is more likely however, that this change is brought about by a change in pH since the pH of the suspension for which GO-COOH was measured was less than that of the suspension used to measure GO-TMA-EG; 5.75 and 6.63, respectively. An increase in pH is associated with a more negative zeta potential and thus can be the explanation for the result obtained.

SEM images of GO-TMA-EG (Figure 28) confirm the presence of Al and show a difference in morphology compared to that of GO-PEG nano-powder.

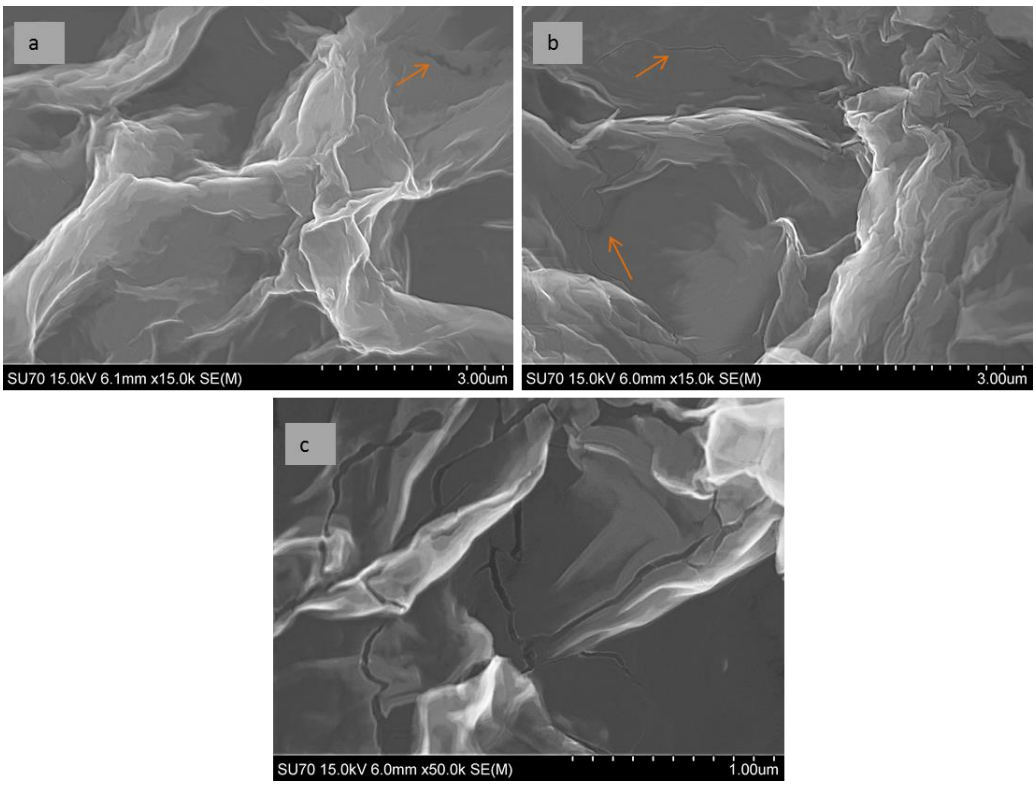

Figure 28: SEM images of GO powder after deposition with TMA and EG. (a) Shows the image before washing; (b) and (c) after washing. The arrows indicate fissures in the material, which are more discernible in (c).

The most apparent difference in the SEM images of GO-PEG and GO-TMA-EG powders is the appearance if fissures in the latter. This can be due to the formation of an alumina coating on the GO, which cracks because of the lack of interfacial contact[54] between the GO and the Al. In this case that may result from the presence of the functional groups on the surface of GO, preventing the maintenance of a continuous

coating. The fissures proliferate after washing because of the removal of the weaker areas of the coating, those between the functional groups.

The EDS spectra for the GO-TMA-EG powder (Figure 29) also confirmed the presence of Al on the composite powder. In addition to GO characteristic elements; C and O, and impurity elements Na, Si and Ca, found in the synthesized GO material, Al is distinctly shown.

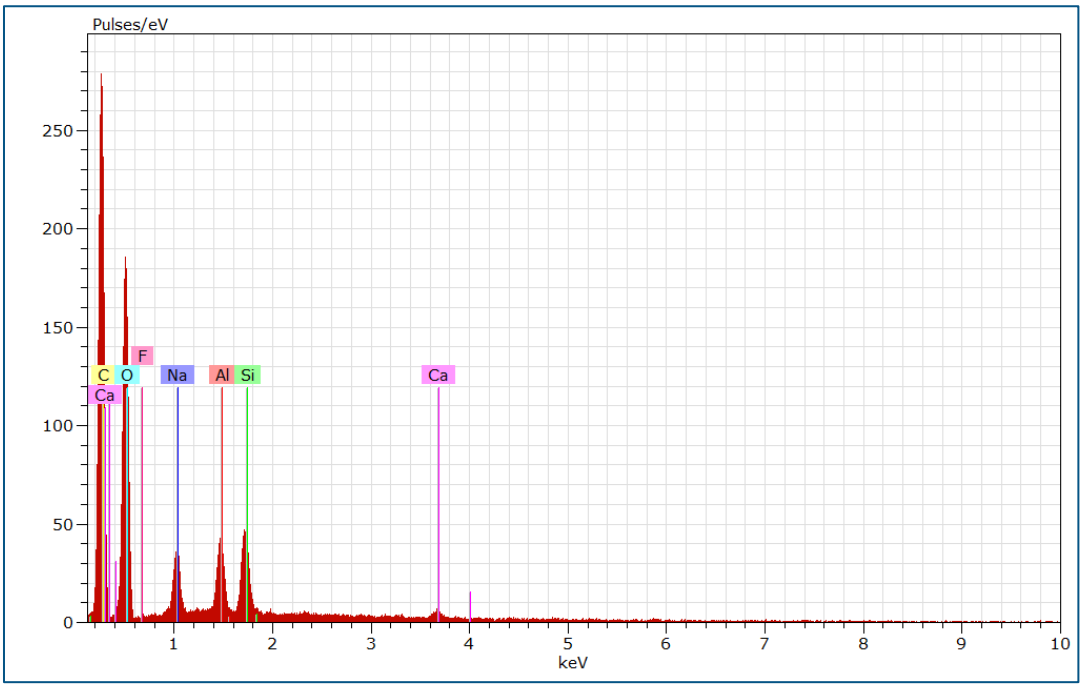

Figure 29: EDS spectra of GO-TMA-EG sample after washing.

The thermal stability of GO-TMA-EG is characterized from TG analysis (Figure 30(a)). The TG curve shows that the presence of Al on the surface of GO shifts the thermal decomposition of the composite material to higher temperatures, compared to that of GO-PEG without exposure to TMA. The curves for the functionalized GO are almost identical up to about 355^{o}C, showing the vaporization of water under 100^{o}C followed by that of GO, around 150^{o}C due to the release of CO, CO_2 and steam from its most labile functional groups[9]. The exothermic peak around 170^{o}C, seen on the DSC curve (Figure 30(b)) was previously shown also to be associated with mass loss of PEG, for the GO-PEG curve. It may be the same for GO-TMA-EG, being linked to the loss of labile groups of EG.

After 355^{o}C, when about 35% of the sample is already lost, thermal decomposition in the GO-TMA-EG composite is shifted to temperatures higher than that of GO-PEG. The start of thermal decomposition of this step occurs around 355^{o}C for GO-PEG and around 450^{o}C for GO-TMA-EG, a shift of about 100^{o}C, explained by the formation of stronger bonds between the functional groups of GO and the Al film. It was previously discussed that this exothermic loss was due to contributions from GO and to a lesser extent, PEG. It seems more likely that it is due mainly to GO for the GO-TMA-EG composite because of

its smaller exothermic peak and evident similarity to that of the DSC curve for GO. The removal of EG therefore occurred in the first step and in the subsequent gradual mass decrease.

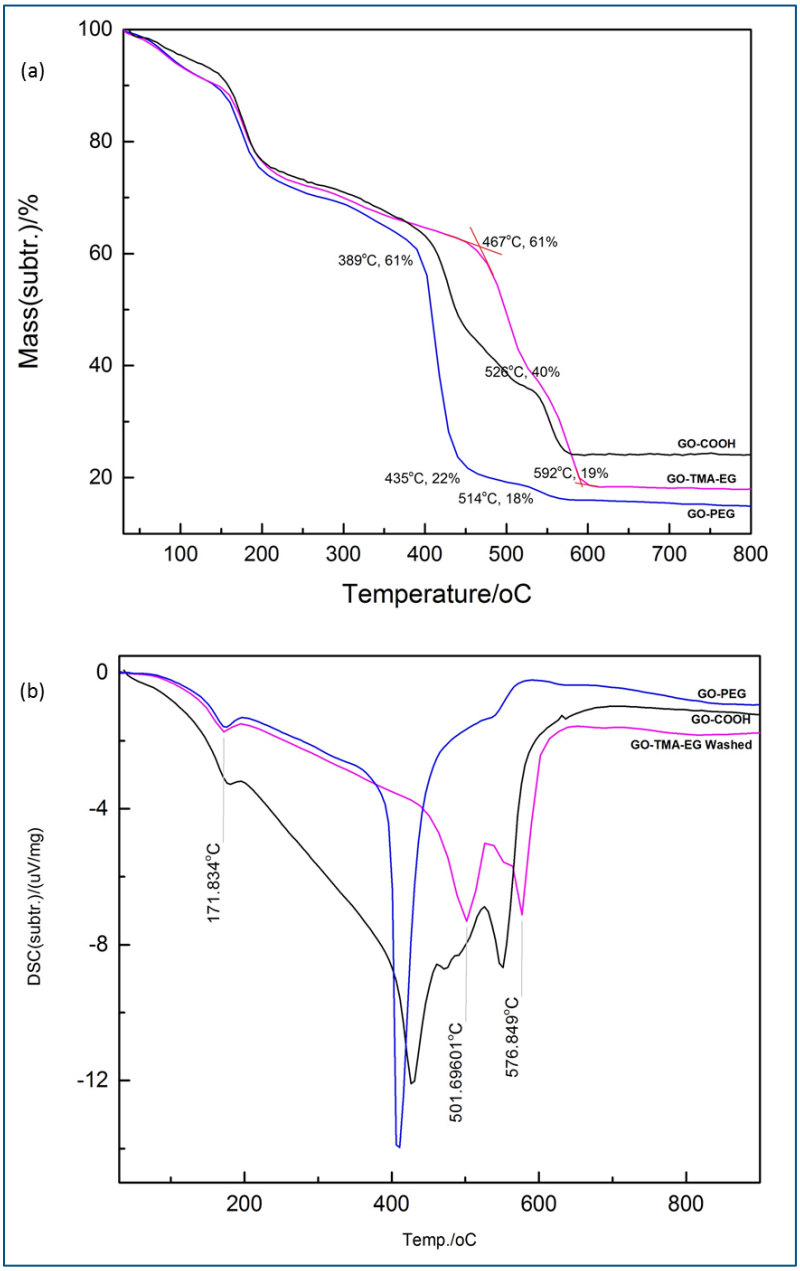

Figure 30: (a) TGA curves of GO, GO-PEG and GO-TMA-EG, (b) DSC of GO, GO-PEG and GO-TMA-EG.

Thermal decomposition of the skeletal carbon structure of GO are also shown at higher temperatures, the main mass loss occurring at 550°C for GO and 576°C for GO-TMA-EG. It was however difficult to determine the quantity of each constituent of the composite powder because of the lack of reference spectra for the precursors and also because of the combined effects describing the decomposition steps. It can therefore be concluded that the presence of Al increases the thermal stability of the GO due to the formation of an Al passivation layer, as identified in the previously discussed SEM images.

CHAPTER 4 Conclusions and Future Prospects

GO was successfully synthesized from the exfoliation of graphite in a modified Hummers' method, and subsequently activated with carboxyl groups using chloroacetic acid. Comparison of the FTIR spectra for graphite, synthesized and activated GO samples showed the presence of characteristic peaks for the C=C GO structure and functional groups of O-H and C-O. Surface activation was indicated by the relative increase in intensity and number of C-O vibrational peaks in the GO-COOH spectrum. The resulting GO sheets recognized an average size of 37.84nm. SEM images demonstrated morphological changes in the rigid graphite parent material compared to the more flexible flake-like appearance of GO.

GO films were shown to be functionalized under rough vacuum conditions via vaporization-condensation reactions using amine-terminated PEG. Evidence of functionalization was determined for the washed samples, suggesting that the deposition resulted in a physical coating on the surface, hindering signals from chemical bonds at surface activated points, which were revealed only after washing away the coating. Errors due to measurement caused by the different FTIR measurement modes used were also determined as a cause of discrepancy between unwashed and washed spectra.

It was observed that covalent attachment of PEG favoured lower temperatures, $80^{o}C$ – $100^{o}C$, shown by the prominence of characteristic peaks around $2923cm^{-1}$ and $2854cm^{-1}$ for asymmetric and symmetric CH_2 groups, as well as those around $1600cm^{-1}$ and $1060cm^{-1}$ for C=O of the amide bond and C-O of the PEG structure, respectively. This made it possible to functionalize GO powder with PEG at $90^{o}C$ in much the same way as the films, the morphology of the nano-powder being conserved in the process.

Dry functionalization of GO powder was also achieved via MLD, using precursors TMA and EG, in an MLD sequence performed at a temperature of $90^{o}C$. FTIR analysis revealed the presence of characteristic EG peaks, with washing confirming covalent bonding. Identification of Al bonds on the spectra was challenging, although the possibility of Al-O-C was reasoned to exist around $1060cm^{-1}$. The presence of Al on GO was indisputably confirmed by SEM and EDS. The deposition parameters were also found to be sufficient for covalent attachment of EG to GO via an Al passivation layer, carried out in under 7 hours.

The results of this experimental research have therefore shown the functionalization of GO-COOH with PEG using a dry route, in under 7hours and with minimal loss of sample, a significant result when compared to the days and even weeks required to achieve this via wet chemical methods.

This work can be continued to better optimize dry functionalization of GO and obtain molecular level control of the polymer. The MLD parameters chosen for control of precursor delivery and purging are exaggerated and could be optimized to obtain greater efficiency of functionalization. Firstly, purging times can be modified to determine the optimal time necessary for the efficient removal of unadsorbed

precursor from the inner flow tube of the reactor. This time would be specific to the precursor and would differ according to the combination of precursors chosen for MLD; an excess of purging will make the process inefficient, while insufficient purging will lead to build up of precursor in the walls of the furnace flow tube and result in contamination of the sample due to secondary reactions. The effect of valve opening times can also be investigated to control the quantity of precursor needed to react with the surface species.

The number of MLD cycles in another parameter that can be modified to optimize this method of dry functionalization. This, like purging times and valve opening times can significantly reduce the time of functionalization. The sequential and self-limiting characteristics of MLD suggests that ideally one cycle should achieve the sequential deposition of the desired molecule, preventing further reactions with the respective surface species once reacted. Measuring the proliferation of the polymer chains would be beneficial to determine the number of cycles necessary to obtain the desired number of repeating monomer units. As it applies to this particular research, experimentation of sequential exposure of each precursor in one cycle could be further performed to determine the growth of polymers on the GO surface.

In situ characterization techniques can be incorporated with MLD to better understand the reactions occurring in the reactor. FTIR measurements can determine conformity and linearity of growth by monitoring changes in bonding groups for each purging step. The use of an in situ quartz crystal microbalance (QCM) can monitor mass changes, thereby characterizing the growth rate (growth per cycle), allowing verification of polymer growth and controlling the size of the polymer.

Additional techniques of ex situ characterization, on the samples already obtained can be performed to support results of this work. XPS (X-ray Photoelectron Spectroscopy), AFM (Atomic Force Microscopy) and NMR (Nuclear Magnetic Resonance) are all techniques which have been used in published work to characterize MLD films and functionalized GO. They contribute the proficiency for specifically characterizing the surface of GO; showing changes in thickness, surface area coverage, morphology and the composition at surface anchoring sites. Confirmation of the results already obtained by more sensitive techniques will increase their reliability and validity.

Bibliography

(1) Marichy, C.; Pinna, N. Carbon-Nanostructures Coated/decorated by Atomic Layer Deposition: Growth and Applications. *Coord. Chem. Rev.* **2013**, *257*, 3232–3253.

(2) Zhu, Y.; Murali, S.; Cai, W.; Li, X.; Suk, J. W.; Potts, J. R.; Ruoff, R. S. Graphene and Graphene Oxide: Synthesis, Properties, and Applications. *Adv Mater* **2010**, *22*, 3906–3924.

(3) Choi, W.; Lahiri, I.; Seelaboyina, R.; Kang, Y. S. Synthesis of Graphene and Its Applications: A Review. *Crit. Rev. Solid State Mater. Sci.* **2010**, *35*, 52–71.

(4) Wassei, J. K.; Kaner, R. B. Oh the Places You'll Go with Graphene. *Acc. Chem. Res.* **2013**, *46*, 2244–2253.

(5) Luo, J.; Kim, J.; Huang, J. Material Processing of Chemically Modified Graphene: Some Challenges and Solutions. *Acc. Chem. Res.* **2013**, *46*, 2225–2234.

(6) Dreyer, D. R.; Park, S.; Bielawski, C. W.; Ruoff, R. S. The Chemistry of Graphene Oxide. *Chem. Soc. Rev.* **2010**, *39*, 228–240.

(7) Gonçalves, G.; Vila, M.; Portolés, M. T.; Vallet-Regi, M.; Gracio, J.; Marques, P. A. a P. Nano-Graphene Oxide: A Potential Multifunctional Platform for Cancer Therapy. *Adv. Healthc. Mater.* **2013**, *2*, 1072–1090.

(8) Hummers, W. S.; Offeman, R. E. Preparation of Graphitic Oxide. *J. Am. Chem. Soc.* **1958**, *80*, 1339–1339.

(9) Marcano, D. C.; Kosynkin, D. V; Berlin, J. M.; Sinitskii, a; Sun, Z. Z.; Slesarev, a; Alemany, L. B.; Lu, W.; Tour, J. M. Improved Synthesis of Graphene Oxide. *ACS Nano* **2010**, *4*, 4806–4814.

(10) Soldano, C.; Mahmood, A.; Dujardin, E. Production, Properties and Potential of Graphene. *Carbon N. Y.* **2010**, *48*, 2127–2150.

(11) Bosch-Navarro, C.; Coronado, E.; Martí-Gastaldo, C.; Sánchez-Royo, J. F.; Gómez, M. G. Influence of the pH on the Synthesis of Reduced Graphene Oxide under Hydrothermal Conditions. *Nanoscale* **2012**, *4*, 3977.

(12) Imani, R.; Emami, S. H.; Faghihi, S. Nano-Graphene Oxide Carboxylation for Efficient Bioconjugation Applications: A Quantitative Optimization Approach. *J. Nanoparticle Res.* **2015**, *17*.

(13) Jokerst, J. V; Lobovkina, T.; Zare, R. N.; Gambhir, S. S. Nanoparticle PEGylation for Imaging and Therapy. *Nanomedicine (Lond).* **2011**, *6*, 715–728.

(14) Roberts, M. J.; Bentley, M. D.; Harris, J. M. Chemistry for Peptide and Protein PEGylation. *Adv. Drug Deliv. Rev.* **2012**, *64*, 116–127.

(15) Yang, K.; Zhang, S.; Zhang, G.; Sun, X.; Lee, S. T.; Liu, Z. Graphene in Mice: Ultrahigh in Vivo Tumor Uptake and Efficient Photothermal Therapy. *Nano Lett* **2010**, *10*, 3318–3323.

(16) Vila, M.; Matesanz, M. C.; Goncalves, G.; Feito, M. J.; Linares, J.; Marques, P. A.; Portoles, M. T.; Vallet-Regi, M. Triggering Cell Death by Nanographene Oxide Mediated Hyperthermia. *Nanotechnology* **2014**, *25*, 35101.

(17) Morales-Narváez, E.; Merkoçi, A. Graphene Oxide as an Optical Biosensing Platform. *Adv. Mater.* **2012**, *24*, 3298–3308.

(18) Huang, P.-J. J.; Liu, J. DNA-Length-Dependent Fluorescence Signaling on Graphene Oxide Surface. *Small* **2012**, *8*, 977–983.

(19) Liu, Z.; Robinson, J. T.; Sun, X.; Dai, H. PEGylated Nano-Graphene Oxide for Delivery of Water Insoluble Cancer Drugs. *J Am Chem Soc* **2008**, *130*, 10876–10877.

(20) Zhao, X.; Liu, P. Biocompatible Graphene Oxide as a Folate Receptor-Targeting Drug Delivery System for the Controlled Release of Anti-Cancer Drugs. *RSC Adv.* **2014**, *4*, 24232–24239.

(21) Yang, K.; Feng, L.; Hong, H.; Cai, W.; Liu, Z. Preparation and Functionalization of Graphene Nanocomposites for Biomedical Applications. *Nat Protoc* **2013**, *8*, 2392–2403.

(22) Vila, M.; Portoles, M. T.; Marques, P. A.; Feito, M. J.; Matesanz, M. C.; Ramirez-Santillan, C.; Goncalves, G.; Cruz, S. M.; Nieto, A.; Vallet-Regi, M. Cell Uptake Survey of Pegylated Nanographene Oxide. *Nanotechnology* **2012**, *23*, 465103.

(23) Thermo Scientific. Easy molecular bonding crosslinking technology https://tools.lifetechnologies.com/content/sfs/brochures/1602163-Crosslinking-Reagents-Handbook.pdf (accessed May 31, 2015).

(24) Liu, Z.; Robinson, J. T.; Sun, X.; Dai, H. PEGylated Nano-Graphene Oxide for Delivery of Water Insoluble Cancer Drugs - Supplementary Information. *J Am Chem Soc* **2008**, *130*, 10876–10877.

(25) Miao, W.; Shim, G.; Lee, S.; Lee, S.; Choe, Y. S.; Oh, Y. K. Safety and Tumor Tissue Accumulation of Pegylated Graphene Oxide Nanosheets for Co-Delivery of Anticancer Drug and Photosensitizer. *Biomaterials* **2013**, *34*, 3402–3410.

(26) Yoon, B.; Seghete, D.; Cavanagh, A. S.; George, S. M. Molecular Layer Deposition of Hybrid Organic−Inorganic Alucone Polymer Films Using a Three-Step ABC Reaction Sequence. *Chem. Mater.* **2009**, *21*, 5365–5374.

(27) Lee, B. H.; Yoon, B.; Abdulagatov, A. I.; Hall, R. a.; George, S. M. Growth and Properties of Hybrid Organic-Inorganic Metalcone Films Using Molecular Layer Deposition Techniques. *Adv. Funct. Mater.* **2013**, *23*, 532–546.

(28) Liang, X.; King, D. M.; Li, P.; George, S. M.; Weimer, A. W. Nanocoating Hybrid Polymer Films on Large Quantities of Cohesive Nanoparticles by Molecular Layer Deposition. *AlChE J.* **2009**, *55*, 1030–1039.

(29) Du, Y.; George, S. M. Molecular Layer Deposition of Nylon 66 Films Examined Using in Situ FTIR Spectroscopy. *J. Phys. Chem. C* **2007**, *111*, 8509–8517.

(30) Yoshimura, T.; Tatsuura, S.; Sotoyama, W. Polymer Films Formed with Monolayer Growth Steps by Molecular Layer Deposition. *Appl. Phys. Lett.* **1991**, *59*, 482.

(31) Dameron, A. A.; Seghete, D.; Burton, B. .; Davidson, S. D.; Cavanagh, A. S.; Bertrand, J. .; George, S. M. Molecular Layer Deposition of Alucone Polymer Films Using Trimethylaluminum and Ethylene Glycol. *Chem. Mater.* **2008**, *20*, 3315–3326.

(32) Wang, L.; Travis, J. J.; Cavanagh, A. S.; Liu, X.; Koenig, S. P.; Huang, P. Y.; George, S. M.; Bunch, J. S. Ultrathin Oxide Films by Atomic Layer Deposition on Graphene. *Nano Lett.* **2012**, *12*, 3706–3710.

(33) McDonnell, S.; Pirkle, A.; Kim, J.; Colombo, L.; Wallace, R. M. Trimethyl-Aluminum and Ozone Interactions with Graphite in Atomic Layer Deposition of Al2O3. *J. Appl. Phys.* **2012**, *112*, 104110.

(34) Pirkle, a; McDonnell, S.; Lee, B.; Kim, J.; Colombo, L.; Wallace, R. M. The Effect of Graphite Surface Condition on the Composition of Al2O3 by Atomic Layer Deposition. *Appl. Phys. Lett.* **2010**, *97*, 82901.

(35) Hsieh, C. Te; Chen, W. Y.; Tzou, D. Y.; Roy, A. K.; Hsiao, H. T. Atomic Layer Deposition of Pt Nanocatalysts on Graphene Oxide Nanosheets for Electro-Oxidation of Formic Acid. *Int. J. Hydrogen Energy* **2012**, *37*, 17837–17843.

(36) Danhier, F.; Ansorena, E.; Silva, J. M.; Coco, R.; Le Breton, A.; Préat, V. PLGA-Based Nanoparticles: An Overview of Biomedical Applications. *J. Control. Release* **2012**, *161*, 505–522.

(37) Khan, M. S.; Vishakante, G. D.; Siddaramaiah H. Gold Nanoparticles: A Paradigm Shift in Biomedical Applications. *Adv. Colloid Interface Sci.* **2013**, *199-200*, 44–58.

(38) Yu, L.; Zhang, Y.; Zhang, B.; Liu, J. Enhanced Antibacterial Activity of Silver Nanoparticles/halloysite Nanotubes/graphene Nanocomposites with Sandwich-like Structure. *Sci. Rep.* **2014**, *4*, 4551.

(39) Peng, S.; Fan, X.; Li, S.; Zhang, J. Green Synthesis and Characterization of Graphite Oxide by Orthogonal Experiment. *J. Chil. Chem. Soc.* **2013**, *58*, 2213–2217.

(40) Kumar, N.; Das, S.; Bernhard, C.; Varma, G. D. Effect of Graphene Oxide Doping on Superconducting Properties of Bulk MgB 2. *Supercond. Sci. Technol.* **2013**, *26*, 095008.

(41) Ciobotaru, C. C.; Damian, C. M.; Matei, E.; Iovu, H.; Xps, X. P. S.; Tga, T. Covalent Functionalization of Graphene Oxide with Cisplatin. *Mater. Plast.* **2014**, *51*, 75–80.

(42) Bourlinos, A. B.; Gournis, D.; Petridis, D.; Szabó, T.; Szeri, A.; Dékány, I. Graphite Oxide: Chemical Reduction to Graphite and Surface Modification with Primary Aliphatic Amines and Amino Acids. *Langmuir* **2003**, *19*, 6050–6055.

(43) Hontoria-Lucas, C.; López-Peinado, A. J.; López-González, J. d. D.; Rojas-Cervantes, M. L.; Martín-Aranda, R. M. Study of Oxygen-Containing Groups in a Series of Graphite Oxides: Physical and Chemical Characterization. *Carbon N. Y.* **1995**, *33*, 1585–1592.

(44) Sun, X.; Liu, Z.; Welsher, K.; Robinson, J. T.; Goodwin, A.; Zaric, S.; Dai, H. Nano-Graphene Oxide for Cellular Imaging and Drug Delivery. **2008**.

(45) Jastrzebska, A. M.; Olszyna, A. R.; Jureczko, J.; Kunicki, A. New Reduced Graphene Oxide/Alumina (RGO/Al2O3) Nanocomposite: Innovative Method of Synthesis and Characterization. *Int. Jounal Appl. Ceram. Technol.* **2013**, 1–7.

(46) Whitby, R. L. D.; Korobeinyk, A.; Gun'ko, V. M.; Busquets, R.; Cundy, A. B.; László, K.; Skubiszewska-Zięba, J.; Leboda, R.; Tombacz, E.; Toth, I. Y.; *et al.* pH-Driven Physicochemical Conformational Changes of Single-Layer Graphene Oxide. *Chem. Commun. (Camb).* **2011**, *47*, 9645–9647.

(47) Stuart, B. *Biological Applications of Infrared Spectroscopy*; Ando, D., Ed.; John Wiley & Sons, 1997.

(48) Wang, C.; Feng, L.; Yang, H.; Xin, G.; Li, W.; Zheng, J.; Tian, W.; Li, X. Graphene Oxide Stabilized Polyethylene Glycol for Heat Storage. *Phys. Chem. Chem. Phys.* **2012**, *14*, 13233.

(49) Ali Umar, M. I.; Yap, C. C.; Awang, R.; Mat Salleh, M.; Yahaya, M. The Effect of Spin-Coated Polyethylene Glycol on the Electrical and Optical Properties of Graphene Film. *Appl. Surf. Sci.* **2014**, *313*, 883–887.

(50) Shameli, K.; Ahmad, M. Bin; Jazayeri, S. D.; Sedaghat, S.; Shabanzadeh, P.; Jahangirian, H.; Mahdavi, M.; Abdollahi, Y. Synthesis and Characterization of Polyethylene Glycol Mediated Silver Nanoparticles by the Green Method. *Int. J. Mol. Sci.* **2012**, *13*, 6639–6650.

(51) Chen, J.; Wang, X.; Chen, T. Facile and Green Reduction of Covalently PEGylated Nanographene Oxide via a "Water-Only" Route for High-Efficiency Photothermal Therapy. *Nanoscale Res. Lett.* **2014**, *9*, 86.

(52) Wu, H.; Lin, K.; Wang, P.; Lin, C.; Yang, H.; Ma, C. M.; Lu, Y.; Jan, T. Polyethylene Glycol-Coated Graphene Oxide Attenuates Antigen-Specific IgE Production and Enhanced Antigen-Induced T-Cell Reactivity in Ovalbumin-Sensitized BALB / c Mice. *Int. J. Nanomedicine* **2014**, *9*, 4257–4266.

(53) Lee, B.; Koo, M. Y.; Jin, S. H.; Kim, K. T.; Hong, S. H. Simultaneous Strengthening and Toughening of Reduced Graphene Oxide/alumina Composites Fabricated by Molecular-Level Mixing Process. *Carbon N. Y.* **2014**, *78*, 212–219.

(54) Kim, H. J.; Lee, S.-M.; Oh, Y.-S.; Yang, Y.-H.; Lim, Y. S.; Yoon, D. H.; Lee, C.; Kim, J.-Y.; Ruoff, R. S. Unoxidized Graphene/alumina Nanocomposite: Fracture- and Wear-Resistance Effects of Graphene on Alumina Matrix. *Sci. Rep.* **2014**, *4*, 5176.